

問題である。抗 α IIb モノクローナル抗体である SZ22 が抗 LIBS 抗体であることは、平成 20 年度に報告した。この抗体の epitope は α IIb 鎖の脚部を構成する calf-2 ドメインに局在することがわかっている。図 6 に示したように SZ22 の α IIb β 3 への結合は RGD ペプチドの濃度に依存して増加した。一方、H12-vesicle は 551(+), 555(+)) ともに SZ22 結合の有意な増加は起こさなかった。しかし vesicle の濃度が極端に高い場合には、僅かではあるが増加する傾向がみられた。興味あることに、生理的濃度のフィブリノーゲンは SZ22 の結合を著明に減少させた (図 7)。この効果が SZ22 だけにみられるのか、他の抗 LIBS 抗体に共通にみられるのかは明らかではない。低活性型 α IIb β 3 と H12-vesicle の結合がフィブリノーゲンによって阻害されたことを考えると、血管内では α IIb β 3 の構造変化が起こりにくい状況にあると思われる。以上の結果から、555(+)) は 551(+)) に比べて優れた血小板結合作用をもつと期待されるが、 α IIb β 3 の構造変化を惹起させる効果は観察されず、安全性は保たれていると考えられる。

平成 20 年度に報告した 551(+)) と α IIb β 3 の PT25-2 存在下での結合の Kd 値、Bmax 値はそれぞれ 0.40 ± 0.07 mg/ml、 77.5 ± 3.98 、551(+)) と Q595NTT 変異株との結合の Kd 値、Bmax 値はそれぞれ 0.26 ± 0.04 mg/ml、 75.1 ± 2.92 であった。Bmax 値の比較は、ロットによって DiOC18 標識 551(+)) の非活性が同一ではない可能性が高いため困難である。しかし、この Kd 値は今回の測定結果の 20~50% と低く、ロットによって結合親和性が大きく異なることを示唆している。原因としてはリポソーム調整の過程で機能に差が出る他に、DiOC18 標識の過程で機能に影響が出る可能性が考えられる。DiOC18 標識が均一に行われていないことも考慮すると、標識に依存しない機能の測

定系を確立し、ロットによる機能のバラツキを評価することが必要であろう。

結論

H12-vesicle のリポソーム脂質膜組成を調整することにより、止血機能の最適化を行うことができると考えられた。止血機能の基礎的な評価を行う上で、標識に依存しない測定系の確立が必要である。

G. 研究発表

1 論文発表 : 1) Tetsuji Kamata, Makoto Handa, Sonomi Ito, Yukiko Sato, Toshimitsu Ohtani, Yohko Kawai, Yasuo Ikeda, and Sadakazu Aiso: Structural Requirements for Activation in α IIb β 3 Integrin. *J.Biol.Chem.* ; 285(49):38428-37, 2010.

2 学会発表: Tetsuji Kamata, Makoto Handa, Yohko Kawai, Yasuo Ikeda and Sadakazu Aiso: Regulatory Role of the Extracellular a-Tail/b-Tail Interaction in α IIb β 3 Integrin Activation. The 52nd ASH Annual Meeting and Exposition. Orlando, FL, December 4-7, 2010

H. 知的財産権の出願・登録 : 無し。

Ⅲ. 研究成果の刊行に関する一覧表

研究成果の刊行に関する一覧表

雑誌

発表者氏名	論文タイトル名	発表誌名	巻(号)	ページ	出版年
Yoshida H, Okamura Y, Watanabe N, <u>Ikeda Y</u> , <u>Handa M</u> .	Shear-dependent suppression of platelet thrombus formation by phosphodiesterase 3 inhibition requires low levels of concomitant Gs-coupled receptor stimulation	<i>Thromb Haemost.</i>	105 (3)	487-495	2011
Shono S, <u>Kinoshita M</u> , Takase B, Nogami Y, Kaneda S, Ishihara M, Saitoh D, Kikuchi M, Seki S.	Intraosseous transfusion with liposome-encapsulated hemoglobin improves mouse survival after hypohemoglobinemic shock without scavenging nitric oxide	<i>Shock.</i>	35 (1)	45-52	2011
Taguchi K, Ogaki S, Watanabe H, Kadowaki D, Sakai H, Kobayashi K, Horinouchi H, <u>Maruyama T</u> , Otagiri M.	Fluid Resuscitation with Hemoglobin Vesicles Prevents Escherichia coli Growth via Complement Activation in a Hemorrhagic Shock Rat Model	<i>J Pharmacol Exp Ther.</i>	337 (1)	201-208	2011
Taguchi K, Iwao Y, Watanabe H, Kadowaki D, Sakai H, Kobayashi K, Horinouchi H, <u>Maruyama T</u> , Otagiri M.	Repeated injection of high doses of hemoglobin-encapsulated liposomes (hemoglobin vesicles) induces accelerated blood clearance in a hemorrhagic shock rat model	<i>Drug Metab Dispos.</i>	39 (3)	484-489	2011
Taguchi K, Miyasato M, Watanabe H, Sakai H, Tsuchida E, Horinouchi H, Kobayashi K, <u>Maruyama T</u> , Otagiri M.	Alteration in the pharmacokinetics of hemoglobin-vesicles in a rat model of chronic liver cirrhosis is associated with Kupffer cell phagocyte activity	<i>J Pharm Sci.</i>	100 (2)	775-783	2011
Okamura, Y., Katsuno, S., Suzuki, H., <u>Maruyama, H</u> , <u>Handa, M.</u> , <u>Ikeda, Y.</u> and <u>Takeoka, S.</u>	Release abilities of adenosine diphosphate from phospholipid vesicles with different membrane properties and their hemostatic effects as a platelet substitute	<i>J. Controlled Release</i>	148 (3)	373-379	2010
Okamura, Y., Eto, K., <u>Maruyama, H.</u> , <u>Handa, M.</u> , <u>Ikeda, Y.</u> , and <u>Takeoka, S.</u>	Visualization of Liposomes Carrying Fibrinogen γ -Chain Dodecapeptide Accumulated to Sites of Vascular Injury Using Computed Tomography	<i>Nanomedicine</i>	6 (2)	391-396	2010
Nogami, Y., Takase, B., <u>Kinoshita, M.</u> , Shono, S., Kaneda, S., Ishihara, M., Kikuchi, M., Maehara, T.	Characteristic changes in heart rate variability induces during hemorrhagic shock, and effect of liposome-encapsulated hemoglobin in rats	<i>J Arrhythmia</i>	26 (3)	189-198	2010
<u>Kinoshita, M.</u> , Uchida, T., Sato, A., Nakashima, M., Nakashima H., Shono S., Habu, Y., Miyazaki, H., Hiroi, S., and Seki, S.	Characteriation of two F4/80-positive Kupffer cell subsets by their function and phenotype in mice	<i>J. Hepatol.</i>	53 (5)	903-910	2010
Kamata T, <u>Handa M</u> , Ito S, Sato Y, Ohtani T, Kawai Y, <u>Ikeda Y</u> , Aiso S.	Structural requirements for activation in α IIb β 3 integrin	<i>J Biol Chem.</i>	285 (49)	38428-38437	2010

IV. 研究成果の刊行物・別冊

Shear-dependent suppression of platelet thrombus formation by phosphodiesterase 3 inhibition requires low levels of concomitant Gs-coupled receptor stimulation

Hideo Yoshida^{1,3}; Yosuke Okamura^{2,3}; Naohide Watanabe³; Yasuo Ikeda²; Makoto Handa³

¹Tokyo New Drug Research Laboratories, Kowa Company, Ltd., Tokyo, Japan; ²Department of Life Science and Medical Bioscience, Graduate School of Advanced Science and Engineering, Waseda University, Tokyo, Japan; ³Departments of Transfusion Medicine & Cell Therapy, School of Medicine, Keio University, Tokyo, Japan

Summary

Phosphodiesterase (PDE)3 inhibitors exert potent antiplatelet effects through maintaining elevated intracellular cyclic adenosine monophosphate levels, but do not prolong bleeding time. To resolve this discrepancy, we hypothesised that PDE3 inhibitors effectively suppress shear-induced platelet thrombus formation initiated by the interaction of the platelet receptor GPIIb/IIIa with its ligand, von Willebrand factor (VWF), since arterial thrombosis is more dependent on shear stress as compared with haemostatic plug formation. To test the hypothesis, we compared the *in vitro* effects of K-134 (a PDE3 inhibitor), tirofiban (a GPIIb/IIIa inhibitor) and acetylsalicylic acid (ASA) on ristocetin-induced platelet aggregation and platelet thrombus formation on VWF or collagen surfaces under flow conditions. K-134 inhibited GPIIb/IIIa-dependent platelet aggregation to the same extent as tirofiban and more potently than ASA. Likewise, K-134 and tirofiban effectively inhibited

stable platelet thrombus formation (platelet firm adhesion and subsequent aggregation) on the VWF or collagen surface under high shear, but ASA only inhibited aggregation. Notably, inhibition by K-134 became evident only when a low concentration of PGE1 was present. These inhibitors did not block shear-induced initial platelet contact with VWF via GPIIb/IIIa. In contrast, under low shear, the inhibitory effects of K-134 on platelet aggregation on the collagen surface were lower than tirofiban or ASA. The observed shear-dependent suppression of platelet thrombus formation by PDE3 inhibitor in the presence of low levels of adenylyl cyclase stimulator may contribute to high therapeutic benefit with low risk of bleeding.

Keywords

Phosphodiesterase 3 inhibitor, GPIIb/IIIa, VWF, shear-induced platelet thrombus formation, PGE1

Correspondence to:

Makoto Handa
Department of Transfusion Medicine & Cell Therapy
School of Medicine, Keio University
35 Shinanomachi, Shinjuku-ku, Tokyo 160-8582, Japan
Tel.: +81 3 3353 1211 (ext. 62113), Fax +81 3 3353 9706
E-mail: mhanda@sc.itc.keio.ac.jp

Received: July 10, 2010

Accepted after major revision: November 25, 2010

Prepublished online: December 6, 2010

doi:10.1160/TH10-07-0439

Thromb Haemost 2011; 105: 487–495

Introduction

In platelets, cyclic adenosine monophosphate (cAMP) is a versatile negative regulator of key signalling pathways including Ca^{2+} mobilisation and integrin $\alpha IIb\beta 3$ (glycoprotein (GP)IIb/IIIa) activation, virtually through serine/threonine phosphorylation by the cAMP-dependent protein kinase (PK)A. The cAMP is synthesised from adenosine triphosphate (ATP) by adenylyl cyclase (AC), activated by Gs-coupled receptor stimulation with endogenous agonists such as prostaglandin (PG)I₂ (also known as prostacyclin) or adenosine, and is degraded to 5'-AMP by cyclic guanosine monophosphate (cGMP)-inhibited cAMP phosphodiesterase (PDE)3. As a result, cAMP concentrations in platelets are regulated by the activity balance between AC and PDE3 (1). In fact, a prominent functional synergy exists *in vitro* and *ex vivo* between AC stimulation (e.g. by the PGI₂ analogue PGE1) and PDE3 inhibition (e.g. by the PDE3 inhibitor cilostazol) to suppress platelet activation (1).

Cilostazol is the only PDE3 inhibitor to date approved for clinical use to manage intermittent claudication in patients with peripheral

arterial disease (PAD) (2), and has been shown to inhibit agonist-induced human platelet aggregation *ex vivo* as effectively as the cyclooxygenase inhibitor acetylsalicylic acid (ASA) and the P2Y₁₂ inhibitor clopidogrel (3). Although use of ASA or clopidogrel is complicated by an increased risk of bleeding, cilostazol does not prolong human bleeding time (3, 4), and the risk of haemorrhage associated with treatment is quite low (5, 6). To clarify this discrepancy, we hypothesised that PDE3 inhibitors suppress platelet thrombus formation in a shear-dependent manner, since pathological thrombus at injured arterioles or stenosed arteries is more dependent on high shear stress than physiological haemostatic plug formation. Thrombus formation on von Willebrand factor (VWF) and collagen surfaces under high shear requires association of platelet GPIIb/IIIa with the A1 domain of VWF (7, 8), and GPIIb/IIIa engagement itself activates GPIIb/IIIa independently of other receptors (9). Conversely, under low shear, direct platelet binding to collagen via GPVI, and platelet-to-platelet crosslinking via GPIIb/IIIa and fibrinogen are functionally significant in thrombus formation on collagen (10, 11), whereas GPIIb/IIIa is not necessarily required (8).

Therefore, to test the aforementioned hypothesis, we explored the effect of PDE3 inhibition both on platelet aggregation induced by ristocetin, a non-physiological inducer of VWF binding to GPIIb α and on platelet thrombus formation on a VWF or collagen surface under flow conditions at wall shear rates of 150 s⁻¹ (low shear) or 1,500 s⁻¹ (high shear) by utilising parallel plate flow chambers *in vitro*. Cilostazol is not appropriate for *in vitro* experiments to deduce its clinical effect because its active metabolites also play major roles in its pharmacological effects on human (12). Cilostazol neither increases cAMP levels of human platelets nor inhibits shear stress-induced platelet aggregation at therapeutic concentration in the absence of Gs stimulator *in vitro* (13). Moreover, the specificity of cilostazol is less selective for PDE3 isozyme (14). Hence, to specifically evaluate the effect of PDE3 inhibition on platelet function *in vitro*, we used a more potent and selective PDE3 inhibitor, K-134 (6-(3-(3-cyclopropyl-3-(2-hydroxycyclohexyl)ureido)propoxy)-2(1H)-quinolinone, also known as OPC-33509), which is a cilostazol analogue but is not a pro-drug (14, 15). While IC₅₀ of cilostazol towards PDE2, PDE3A and PDE5 are 45.2, 0.20 and 4.4 μ M, respectively, those of K-134 are >300, 0.10 and 12.1 μ M, respectively (14). Here, we demonstrated that the K-134 effectively suppressed *in vitro* platelet thrombus formation under flow conditions in a more shear-dependent manner than ASA or the GPIIb/IIIa inhibitor tirofiban, and the effect of K-134 was apparent only in the presence of a low concentration of the AC stimulator PGE1. We propose that our data indicate a mechanism whereby PDE3 inhibition exhibits efficient antiplatelet effects on arterial thrombosis with a minimal impact on primary haemostasis.

Materials and methods

Antiplatelet reagents

The PDE3 inhibitors K-134 and cilostazol were obtained from Kowa (Tokyo, Japan). The GPIIb/IIIa inhibitor tirofiban was purchased from Toronto Research Chemicals (Toronto, Canada). The cyclooxygenase inhibitor ASA, Arg-Gly-Asp-Ser (RGDS) peptides (inhibitors of integrins with RGD binding sites), and forskolin (an AC activator) were from Sigma-Aldrich (St Louis, MO, USA). These reagents were dissolved in dimethyl sulfoxide (DMSO). PGE1 was purchased from Cayman Chemical (Ann Arbor, MI, USA) and dissolved in ethanol (EtOH). An inhibitory mouse monoclonal antibody against human GPIIb α , GUR83-35, was obtained from Takara Bio (Shiga, Japan), and the isotype-matched control mouse IgG1 was purchased from SIGMA-Aldrich. The selection of K-134 concentrations is based on the phase-I study and non-clinical study, in which K-134 treatment with a maximal serum concentration of 1–5 μ M showed antiplatelet effects on human *ex vivo* and beneficial effects in a rat model of thrombosis or ischaemia (manuscript in preparation).

Blood sampling

After obtaining informed consent according to the Declaration of Helsinki, blood was collected from the antecubital vein of healthy, medication-free volunteers through a 21-gauge needle and was anticoagulated with D-phenylalanyl-L-prolyl-L-arginine chloromethyl ketone dihydrochloride (PPACK; Calbiochem, San Diego, CA, USA) (final concentration (fc), 40 μ M) or a 10% volume of 3.8% (w/v) sodium citrate. Platelet-rich plasma (PRP) was prepared by centrifugation (100 g, 15 minutes [min], 22°C) of blood, and the platelet count was adjusted to 2.0 $\times 10^5/\mu$ l with platelet-poor plasma prepared by centrifugation (2,200 g, 10 min, 22°C) for agonist-induced platelet aggregation assay. The platelet concentration was determined using an automated haematology analyzer (K-4500; Sysmex, Kobe, Japan).

Agonist-induced platelet aggregation

PPACK-anticoagulated PRP was incubated with antiplatelet agents with or without 6 nM PGE1 at 37°C for 2 min and stimulated with adenosine diphosphate (ADP) (fc, 10 μ M; MC Medical, Tokyo, Japan) or collagen (fc, 1.75–2.75 μ g/ml; Chronolog, Havertown, PA, USA). ADP- or collagen-induced platelet aggregation was quantified by measuring maximum aggregation rate (MAR; percent of maximal light transmittance) within 5 min after addition of trigger using an aggregometer (Hema Tracer T-638; Nico Bioscience, Tokyo, Japan) (n=3). All volunteers' PRP samples showed similar dose-response curves for ADP (EC₅₀: about 5 μ M, MAR induced by 10 μ M ADP: 55–65%). The concentration of collagen was adjusted to give the EC₈₅. Ristocetin-induced platelet aggregation (RIPA) was performed by adding ristocetin solution (fc, 1.5 mg/ml; Sigma-Aldrich) to citrated PRP after incubation with antiplatelet agents at 37°C for 5 min. The effects of antiplatelet agents on RIPA were evaluated by aggregation rates at 10 min after addition of trigger. All volunteers' PRP samples (n=4) showed similar dose-response curves for ristocetin (EC₅₀: about 1.2 mg/ml, aggregation rate at 10 min: > 90%).

Preparation of thrombogenic substrate-coated surfaces

Human VWF (10 μ g/ml; purified from plasma as previously described [16]) and type I collagen derived from porcine tendon (30 μ g/ml; Cellmatrix Type I-A, Nitta Gelatin, Osaka, Japan) were prepared in Dulbecco's phosphate-buffered saline (PBS). Glass coverslips (No. 5, diameter 24 mm, thickness 0.5 mm; Matsunami Glass, Osaka, Japan) were immersed in VWF (22°C, 2.5 h) or collagen (4°C, 12 h) solution, carefully rinsed with PBS, and then blocked with bovine serum albumin (20 mg/ml; Sigma-Aldrich) in PBS (22°C, >2 h). After additional rinsing with PBS, coverslips were assembled into a parallel plate flow chamber just before perfusion experiments.

Perfusion experiments

PPACK-anticoagulated whole blood (5 ml) was incubated with a fluorescent marker (DiOC₆; Molecular Probes, Eugene, OR, USA) and antiplatelet agents at 37°C for 5 min, then aspirated using a roller pump (Minipulse 3; Gilson, Villiers Le Bel, France) and perfused over thrombogenic substrate-coated glass coverslips at a wall shear rate of 150 or 1,500 s⁻¹ in a recirculating chamber (circulation cycle, 180 s or 18 s, respectively) mounted on an inverted epifluorescence microscope (Eclipse TE300; Nikon, Tokyo, Japan) equipped with a charge-coupled device camera (C2400-80V; Hamamatsu Photonics, Hamamatsu, Japan). These experiments were performed at 37°C and recorded on S-VHS videotape using a video cassette recorder (BR-S662; Victor, Tokyo, Japan), and digital images were captured using an Argus-50 image processor (Hamamatsu Photonics) with fixed contrast and brightness. The percentage of total area covered with platelets (designated as surface coverage) and the mean size of surface-bound platelet aggregates (designated as average platelet aggregate size) were calculated using the Argus-50 software. Surface coverage reflects platelet adhesion to the thrombogenic substrate-coated surface (2-dimensional thrombus growth), while average platelet aggregate size represents the degree of platelet aggregation (3-dimensional thrombus growth) on the surface (17, 18). We chose threshold values (grayness level from 0–255, where 0 is black) of 50 for surface coverage and 200 for average platelet aggregate size, to eliminate background fluorescence and fluorescence of single platelets that do not aggregate, respectively.

Measurement of cAMP and cGMP

Citrated PRP was pre-incubated with K-134 with or without 6 nM PGE1 at 37°C for 5 min, and simulated with ristocetin (fc, 1.5 mg/ml) for 10 min under stirring. Platelet intracellular cAMP and cGMP levels were analysed using an Amersham cAMP/cGMP Biotrak Enzymeimmunoassay system (GE Healthcare, Buckinghamshire, UK) and were presented as a concentration of cAMP or cGMP pmol/10⁸ platelets.

Statistical analysis

Statistical analyses were performed using SAS Preclinical Package version 5.0 software (SAS Institute Japan, Tokyo, Japan).

Results

Effects of PDE3 inhibitors on RIPA

First, we compared the inhibitory effects of the PDE3 inhibitors cilostazol and K-134 with other antiplatelet agents on RIPA *in vitro*.

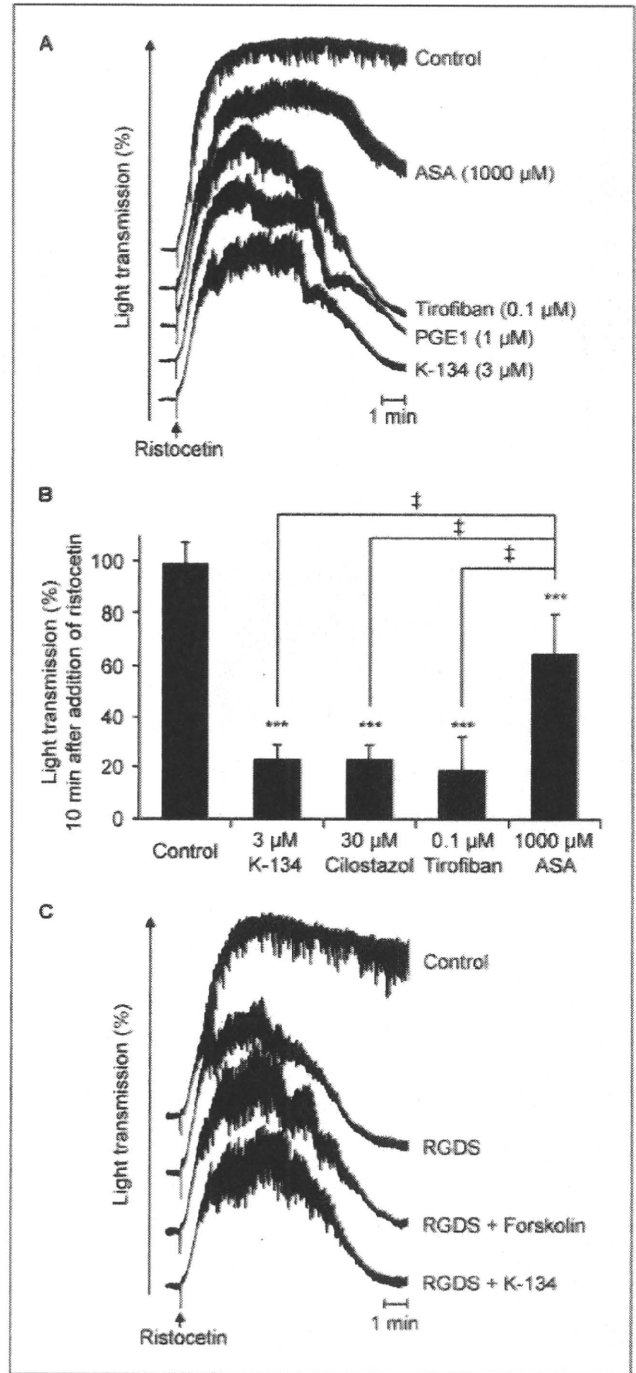


Figure 1: Effects on ristocetin-induced human platelet aggregation. Citrated PRP was preincubated with DMSO (control) or each antiplatelet agent, and stimulated with ristocetin. A, B) Inhibitory effects of agents were estimated by measuring platelet aggregation rate (%) at 10 min after stimulation (n=5). ***p<0.001 vs. control, †p<0.001 vs. ASA group (Tukey’s test). C) The effects of 10 µM forskolin and 10 µM K-134 on ristocetin-induced platelet agglutination were evaluated in the presence of 1 µM RGDS peptides. The agglutination and aggregation curves are representatives of five experiments. Values are mean ± SD.

IC50 (μM)	Ristocetin	Ristocetin (+PGE1)	ADP	ADP (+PGE1)	Collagen	Collagen (+PGE1)
K-134	2.2 (2.0–2.4)	0.77 (0.47–1.1)	6.1 (4.4–8.3)	0.95 (0.76–1.2)	0.74 (0.55–1.0)	0.24 (0.18–0.33)
Cilostazol	22 (18–25)	8.3 (4.8–12)	32 (24–42)	7.3 (6.5–8.2)	6.4 (5.5–7.5)	1.6 (1.4–1.8)
Tirofiban	0.045 (0.011–0.072)	0.061 (0.049–0.072)	0.028 (0.018–0.042)	0.027 (0.021–0.034)	0.022 (0.019–0.026)	0.016 (0.012–0.022)
ASA	>1000	>1000	>1000	>1000	59 (39–91)	55 (40–73)

Table 1: Effects of PDE3 inhibitors on ristocetin-, ADP- or collagen-induced platelet aggregation. Calculated half-maximal inhibitory concentration (IC₅₀) values are expressed as the mean from 3–4 human volunteers. Values in parentheses indicate 95% confidence intervals.

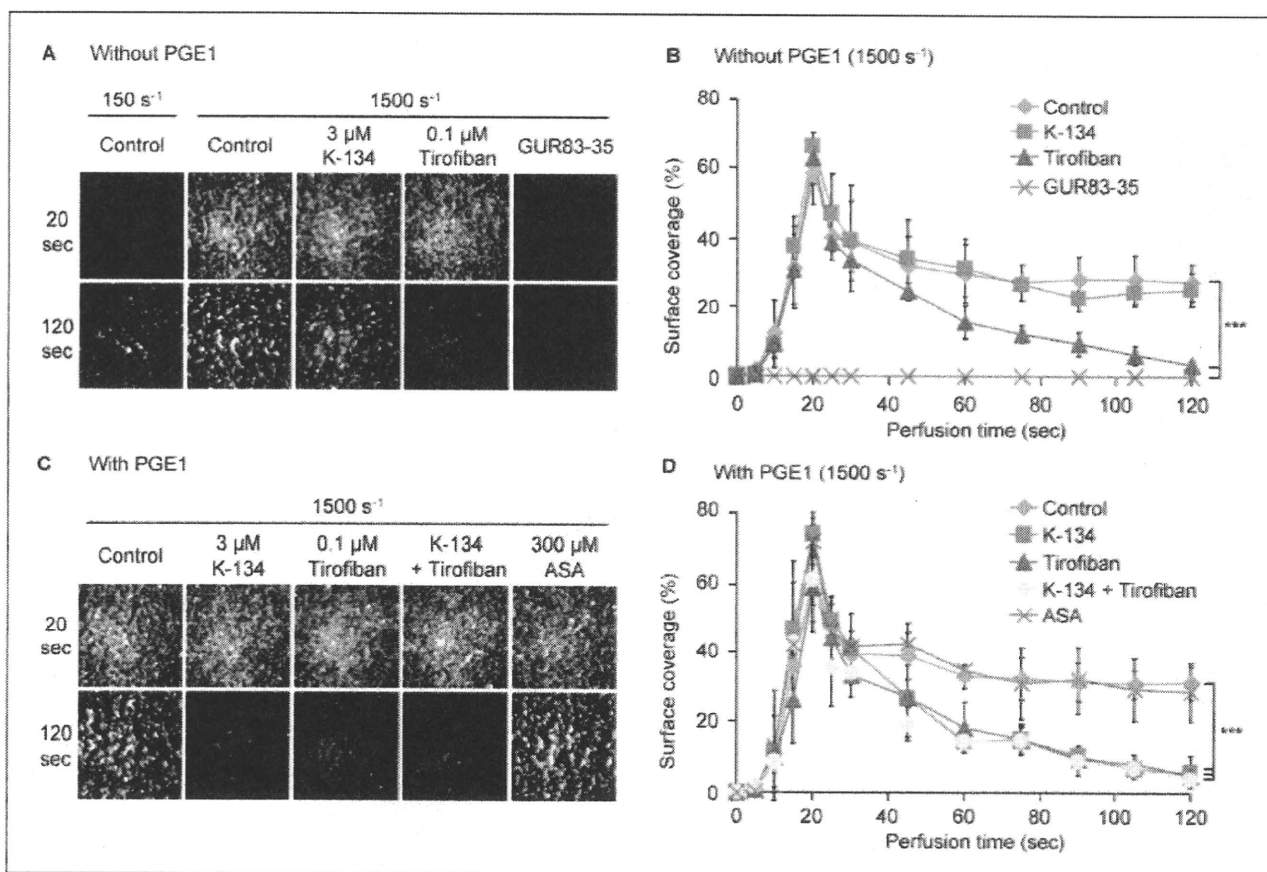


Figure 2: Effects on thrombus formation on a VWF surface under flow. PACK-anticoagulated blood was incubated with DiOC6 for platelet visualisation and DMSO (control) or each antiplatelet agent, and perfused over VWF-immobilised glass coverslips in a parallel plate flow chamber at a wall shear rate of 150 s⁻¹ (A) or 1,500 s⁻¹ (A–D) in the absence (A, B) or presence (C, D) of 6 nM PGE1. To confirm the GPIIb/IIIa-dependency of platelet binding to VWF, 15 μg/ml GUR83–35 was used as a GPIIb/IIIa blocking antibody. The effect

of each inhibitor on platelet initial accumulation via GPIIb/IIIa and on subsequent platelet aggregation was evaluated by measuring surface coverage at 0–120 s after initiation of perfusion. A, C) Representative images, corresponding to a 220 × 220 μm area at 20 or 120 s after initiation of perfusion. ***p<0.001 vs. control (Tukey's test was performed at 120 s). Values are mean ± SD (n=6 for control and n=3 for others).

In effect, 3 μM K-134 and 30 μM cilostazol significantly (p<0.001) inhibited RIPA (evaluated at 10 min after addition of trigger) to the same extent as 0.1 μM tirofiban and 1 μM PGE1, and more potently than 1,000 μM ASA (▶ Fig. 1A, B). To explore the effects of PDE3 inhibitor on GPIIb/IIIa-independent platelet aggregation

mediated through direct interaction between VWF and GPIIb/IIIa, PRP was incubated with an integrin-antagonist peptide, RGDS, before ristocetin stimulation. Under such conditions, K-134 caused no change in agglutination extent and the same was true with PGE1 (not shown) and forskolin, which also increases in-

tracellular cAMP levels via direct AC activation (► Fig. 1C). It was found that GUR83–35, a monoclonal antibody against GPIIb/IIIa completely suppressed the agglutination phenomenon (not shown). These results indicate that an intracellular cAMP level heightened by PDE3 inhibition or AC activation is a crucial down-regulator for platelet aggregation via VWF-GPIIb/IIIa-mediated signals, but not for VWF-GPIIb/IIIa interaction itself that is independent of GPIIb/IIIa.

Next, we examined the synergistic effects of concomitant stimulation of AC on the observed PDE3 inhibition of RIPA. Inducible Gs-coupled receptor stimulation by vascular wall-derived PGI₂ or adenosine is thought to be pathologically relevant in the circulation to defend against thrombosis (19, 20). Therefore, to mimic the *in vivo* situation *in vitro*, we conducted aggregation study in the presence of a very low concentration (6 nM) of PGE1. Our preliminary experiments demonstrated that 6 nM PGE1 was close to the optimal concentration that could elevate cAMP levels in the presence of PDE3 inhibitor, but did not affect agonist-induced platelet aggregation in the absence of PDE3 inhibitor (not shown). Indeed, the inhibitory effects of PDE3 inhibitors on not only ADP- or collagen- but also ristocetin-induced platelet aggregation were readily augmented in the presence of 6 nM PGE1 (► Table 1). In contrast, the effects of tirofiban and ASA were unaffected by PGE1. Taken together, these results indicate that similar to other signals stimulated by ADP and collagen under stirring conditions, the GPIIb/IIIa signal elicited by VWF binding is a cAMP-sensitive pathway.

PDE3 inhibition prevents stable platelet thrombus formation on a VWF surface under flow

To further clarify the effect of PDE3 inhibition on VWF-GPIIb/IIIa-mediated platelet activation under physiological conditions, PPACK-anticoagulated blood was perfused over VWF coated onto glass coverslips. Under arterial flow conditions at a high wall shear rate of 1,500 s⁻¹, platelets exhibited rapid and progressive attachment onto the VWF surface with a peak surface coverage of ~70% at 20 s after perfusion (► Fig. 2A, B). Platelets then started to detach over time (possibly due to the unstable platelet adherence induced by recirculating small platelet aggregates), and stable thrombus formation (surface coverage ~30%) was finally constructed by 120 s. In contrast, at a venous wall shear rate of 150 s⁻¹, platelet thrombus tended to grow slowly on the VWF surface with surface coverage of about 10% even at 120 s (► Fig. 2A), and was not completely abolished by the previous addition of GUR83–35 (not shown). The effect of K-134 on platelet thrombus formation was studied under arterial flow conditions (1,500 s⁻¹). Unexpectedly, K-134 at a therapeutic concentration of 3 μM did not affect the whole profile of thrombus formation, while tirofiban showed an apparent inhibitory effect on the second phase of thrombus formation (at 20–120 s). Although tirofiban did not affect the first phase of platelet contact at 0–20 s, GUR83–35 completely blocked this platelet interaction (► Fig. 2A, B) but the isotype-matched

control mouse IgG1 did not show any effect (not shown), indicating that the first phase of the interaction involves GPIIb/IIIa-independent initial contact of platelets onto VWF via GPIIb/IIIa (► Fig. 2A, B). Prominently enough, although 6 nM PGE1 itself had no inhibitory effect on platelet thrombus formation at such low concentration, K-134 showed a potent inhibitory effect on the second phase of platelet interaction in the presence of 6 nM PGE1 (► Fig. 2C, D). The extent of inhibition by K-134 resembled that by tirofiban and no synergic effect from both inhibitors was observed. In contrast, ASA showed no inhibitory effect under these experimental conditions. These results of perfusion experiments thus indicate that under physiological flow conditions, antiplatelet effects by PDE3 inhibition are mediated by elevated cAMP to efficiently block the initial signalling of the VWF-GPIIb/IIIa pathway and subsequent autocrine activation signals, and the inhibitory effect is only significant in the presence of concomitant low level stimulation of AC.

PDE3 inhibition suppresses platelet thrombus formation on a collagen surface in a shear-dependent manner

To evaluate the effect of PDE3 inhibition on platelet thrombus formation mediated simultaneously by both collagen and VWF, we performed perfusion experiments over glass coverslips coated with type I collagen fibrils, to which plasma-derived VWF was expected to adsorb via the A3 domain. Indeed, we observed that platelet thrombus formation on the collagen surface under high shear (1,500 s⁻¹) was completely blocked by anti-GPIIb/IIIa antibody

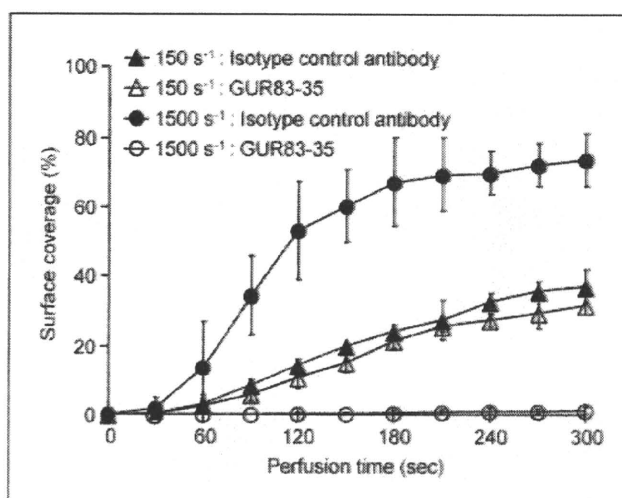


Figure 3: Effect of GPIIb/IIIa blocking on thrombus formation on a collagen surface under flow. Blood treated as described in the legend for Figure 2 was perfused over collagen-immobilised glass coverslips. Effects of GPIIb/IIIa blocking antibody, GUR83–35 (15 μg/ml) on thrombus formation at a wall shear rate of 150 or 1,500 s⁻¹ was evaluated by measuring surface coverage. Values are mean ± SD (n=3).

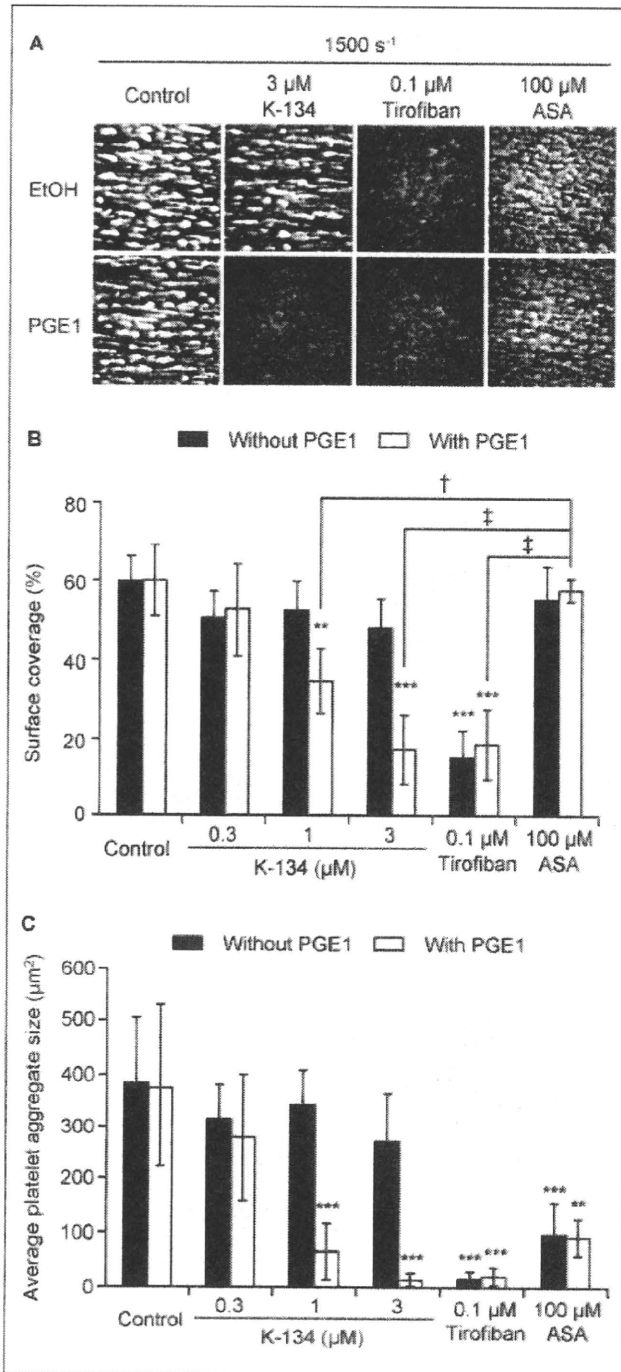


Figure 4: Effects on thrombus formation on a collagen surface under high shear. Blood treated as described in the legend for Figure 2 was perfused over collagen-immobilised glass coverslips at a wall shear rate of 1,500 s⁻¹. A) Representative images corresponding to a 340 x 340 μm area, captured at 270 s after initiation of perfusion. Effects on platelet adhesion and aggregation were evaluated by measuring surface coverage (B) and average platelet aggregate size (C), respectively. **p<0.01, ***p<0.001 vs. control. †p<0.05, ‡p<0.001 vs. ASA with PGE1 group (Tukey's test). Values are mean ± SD (n=8 for control, n=4 for others).

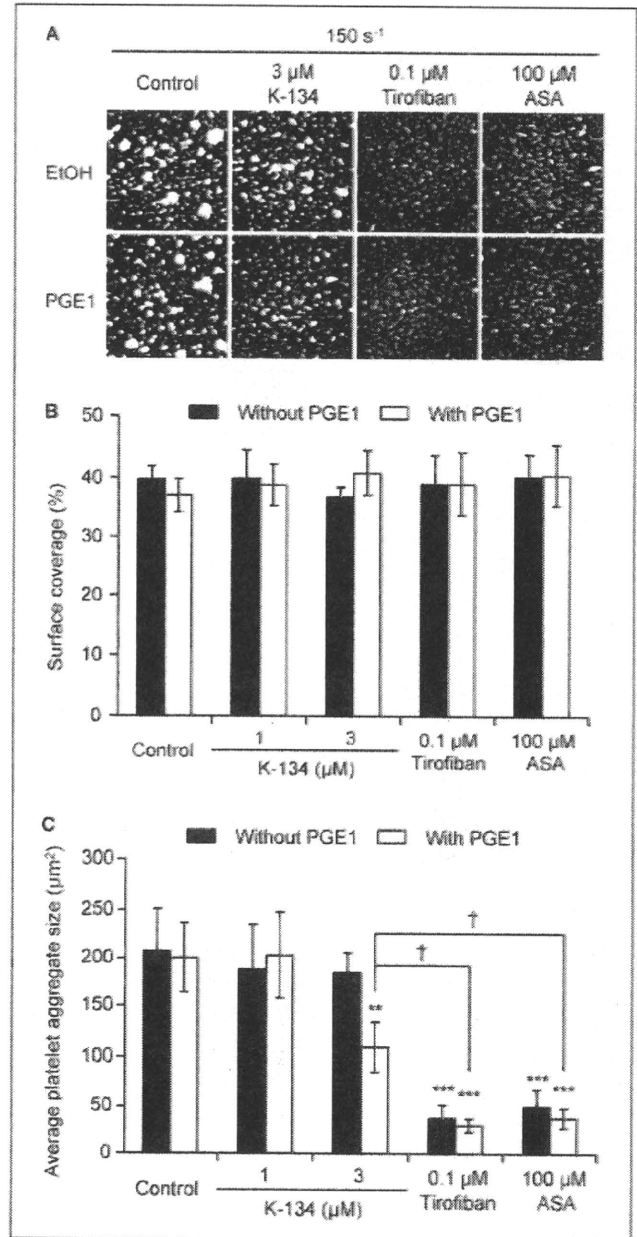


Figure 5: Effects on thrombus formation on a collagen surface under low shear. Blood treated as described in the legend for Figure 2 was perfused over collagen-immobilised glass coverslips at a wall shear rate of 150 s⁻¹. A) Figure shows representative images, corresponding to a 340 x 340 μm area, captured at 270 s after initiation of perfusion. Effects on platelet adhesion and aggregation were evaluated by measuring surface coverage (B) and average platelet aggregate size (C), respectively. **p<0.01, ***p<0.001 vs. control, †p<0.05 vs. 3 μM K-134 with PGE1 group (Tukey's test). Values are mean ± SD (n=4).

GUR83-35, while the antibody was without effect on thrombus formation under low shear (150 s⁻¹) (► Fig. 3). Consistent with previous findings (8, 11), these results indicate that platelet adhesion and subsequent aggregation onto the collagen surface

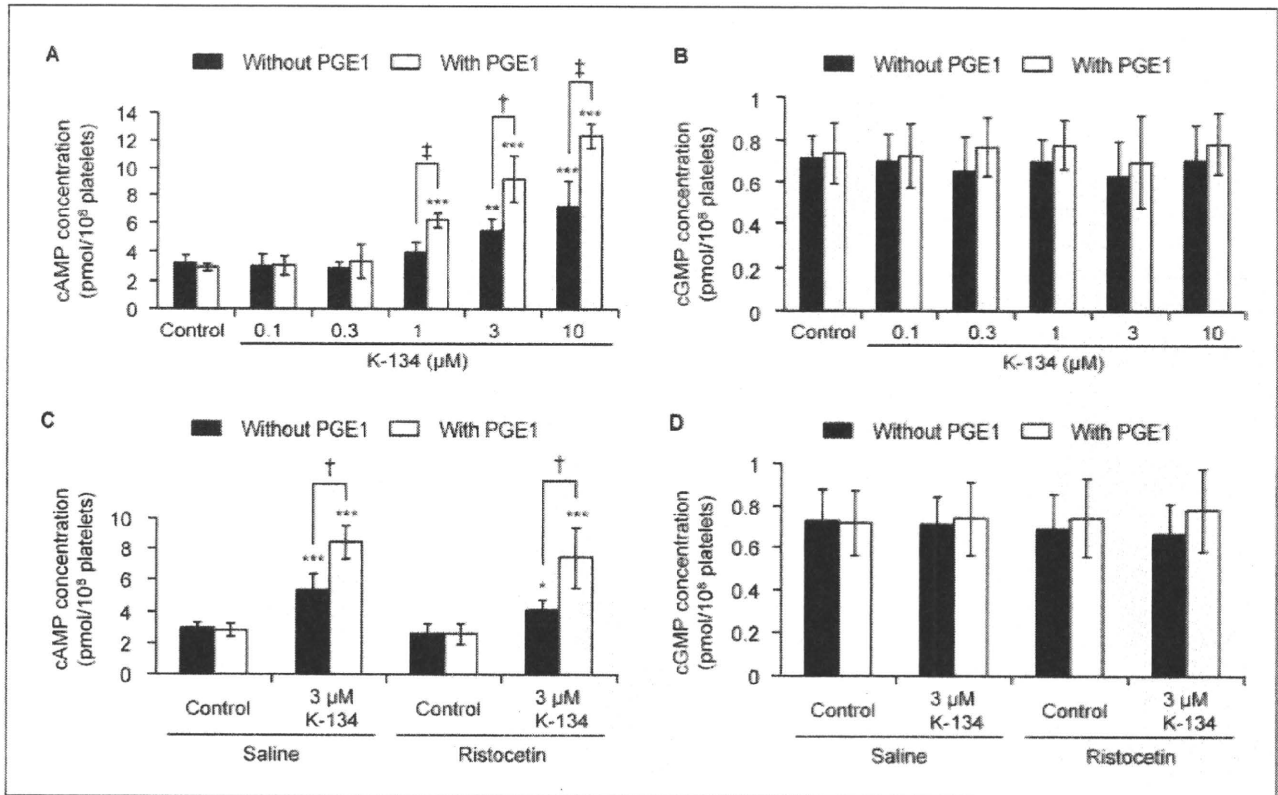


Figure 6: Effects on platelet cAMP and cGMP levels. Citrated PRP was pretreated with DMSO (control) or K-134 with or without 6 nM PGE1 for 5 min, and incubated with ristocetin or vehicle control (saline) for 10 min under stirring. A, B) platelet cAMP and cGMP levels after K-134 pretreatment (n=5).

p<0.01, *p<0.001 vs. control (Dunnett's test), †p<0.01, ‡p<0.001 vs. absence of PGE1 (t-test). C, D) platelet cAMP and cGMP levels after ristocetin-stimulation (n=5). *p<0.05, ***p<0.001 vs. control (Tukey's test). Values are mean ± SD.

under flow conditions is mediated through VWF-GPIb/VIX engagement in a shear rate-dependent manner. We then tested the effects of antiplatelet agents on platelet thrombus formation on the collagen surface under flow conditions. Under high shear, K-134 at least at a therapeutic concentration (~3 μM) was found to be inhibitory only when a low concentration of PGE1 (6 nM) was present (▶ Fig. 4A). In fact, K-134 readily suppressed irreversible platelet adhesion (surface coverage at 270 s) and stable thrombus formation by platelet aggregation (average platelet aggregate size at 270 s) on the collagen surface in a dose-dependent manner in the presence of PGE1 (▶ Fig. 4B, C). Conversely, tirofiban showed potent inhibitory effects on both parameters regardless of the presence or absence of PGE1, whereas ASA was without effects on surface coverage, but effectively (with a weaker effect than K-134 or tirofiban) inhibited platelet aggregate size. In contrast, under low shear, these antiplatelet agents including K-134 did not show any inhibitory effect on platelet surface coverage even in the presence of PGE1 (▶ Fig. 5A, B). Of note, however, was the finding that these agents exhibited significant inhibitory effects on platelet aggregate size and the effect of K-134 became apparent only in the presence of PGE1 (▶ Fig. 5A, C). Also, compared with results obtained under high shear (▶ Fig. 4), the inhibitory effects of K-134

under low shear were significantly weaker than those of 0.1 μM tirofiban or 100 μM ASA (p<0.05).

Taken together, these results indicate that shear-dependent platelet thrombus formation *in vitro* initiated by GPIb/VIX signaling is sensitive to cAMP-mediated regulatory pathways elicited by PDE3 inhibition in the presence of a low concentration of AC stimulator PGE1.

PDE3 inhibition increases platelet intracellular cAMP levels but not cGMP

To ascertain if the inhibitory effect of K-134 are mediated through cAMP or an alternative mechanism, we measured the intracellular cAMP and cGMP levels of platelets treated with K-134. Indeed, K-134 dose-dependently increased platelet cAMP levels but not cGMP, and the effect was potentiated by a low concentration of PGE1 (▶ Fig. 6A, B). Furthermore, the cAMP-elevating effect of K-134 was also maintained in platelets activated by ristocetin under stirring conditions, while K-134 had no effect on cGMP levels (▶ Fig. 6C, D).

Discussion

The GPIb/V/IX engagement with VWF immobilised on the subendothelial collagen surface under arterial flow conditions not only mediates platelet recruitment, but also initiates cellular activation leading to integrin-dependent firm platelet adhesion and aggregation at the site of vascular injury (8, 11). In fact, our findings (► Figs. 1, 2) indicated that the observed suppression of VWF-mediated platelet thrombus formation by PDE3 inhibitors was due to efficient blocking of VWF-induced GPIb/V/IX signalling by elevated cAMP, but was not attributable to the down-regulation of GPIb/V/IX binding affinity with the ligand led by PKA-induced phosphorylation of the GPIb α subunit intracellular domain, which is contrary to previously reported study (21). Consistent with our finding, Mazzucato et al. (18, 22) reported that the magnitude of platelet translocation velocity on immobilised VWF in the presence of cAMP elevating reagents appeared to be the same as that obtained by GPIIb/IIIa blocking in similar perfusion experiments, while raising cAMP levels achieved complete inhibition of intracellular Ca²⁺ elevation and GPIIb/IIIa-mediated stable adhesion and aggregation.

PDE3 inhibitor reduced stable platelet thrombus formation on the collagen surface under high shear in the presence of PGE1 more potently than ASA, but had much lower inhibitory effects under low shear than tirofiban or ASA (► Figs. 4, 5). There is a possible simple explanation as to why PDE3 inhibitor interfered with thrombus formation on the collagen surface in a more shear-dependent manner than tirofiban and ASA: while the secretion-independent signal mediated by VWF bound onto collagen is very sensitive to cAMP, that by collagen through GPVI is resistant to cAMP. In fact, PGE1, but not ADP receptor antagonists and ASA, could obliterate VWF-GPIb/V/IX-mediated initial intracytoplasmic

Ca²⁺ oscillation (18). Moreover, cAMP analog strongly blocked GPIIb/IIIa activation induced by the dimeric VWF A1 domain (through GPIb/V/IX) in the presence of inhibitors of autocrine signalling through ADP and thromboxane A₂ (TXA₂) receptors (9). In addition, Shaun P. Jackson's group reported that platelet adhesion to VWF under high shear (at 600 and 1,800 s⁻¹) was not dependent on either ADP or TXA₂ (23). A primary collagen receptor of platelets is GPVI, which activates c-Src and Syk kinases leading to full cellular activation. In fact, tyrosine phosphorylation of these kinases induced by an anti-GPVI antibody or collagen was not abrogated with PGI₂ treatment (24). Also, marked elevation of cAMP by forskolin reportedly did not inhibit collagen-induced and secretion-independent signalling events including protein-tyrosine phosphorylation, polyphosphoinositide liberation and granular secretion (25). In contrast, GP IV-mediated platelet aggregation (which is secretion-dependent) was completely inhibited by cAMP-elevating agents (24). Thus our findings were consistent with the fact that stable platelet thrombus formation on collagen under high shear is dependent on GPIb/V/IX signalling triggered by VWF and that under low shear that is mediated by GP VI signalling triggered by collagen itself (8, 10, 23).

Gs stimulation with PGE1 or adenosine and PDE3 inhibition synergistically accumulate cAMP to suppress platelet activation (1, 20). In fact, our results indicated that the observed antiplatelet effects of K-134 are most likely to be due to cAMP rather than to cGMP elevation (► Fig. 6). Although K-134 alone potently inhibited VWF-dependent platelet aggregation induced by ristocetin (► Fig. 1A, B), the inhibitory effect was readily enhanced by a low level of Gs stimulation with 6 nM PGE1 (► Table 1). Notably enough, however, an absolute requirement of PGE1 was observed with K-134 at the therapeutic concentrations needed to inhibit VWF-dependent platelet thrombus formation under flow conditions (► Figs. 2, 4). This discrepancy may be due to difference in threshold level of cAMP required to block intracellular signalling: one is ADP- and TXA₂-dependent GPIIb/IIIa activation pathway downstream of VWF-GPIb/V/IX interaction induced by ristocetin (aggregometer studies) and the other is secretion-independent integrin activation pathway induced by shear (flow chamber studies) ([23, 26] and ► Figs. 1, 2, 6). Thus, our *in vitro* findings obtained under physiological flow conditions raised the notion that VWF-induced platelet thrombus formation may be efficiently blocked by PDE3 inhibitor under *in vivo* conditions where the endogenous Gs stimulators (PGI₂ and adenosine) are up-regulated. As a matter of fact, considerable amounts of PGI₂ were reportedly produced locally in response to mural platelet thrombus formation on de-endothelialised arterial wall (19). In addition, adenosine was released in hypoxic tissues during ischaemia and exerted ischaemic preconditioning effects (27, 28). Since both of these substances have very short biological lives *in vitro*, the stable PGI₂ analogue, PGE1 may instead mimic the *in vivo* supporting effects on PDE3 inhibitor-driven suppression of VWF-dependent platelet thrombus formation under arterial shear conditions. Meanwhile, we speculated that there is no feasibility of clinical use of combined PDE3 inhibitor and Gs stimulator, since long-term administration of Gs stimulator leads to decreased sensitivity of human platelets to the drug (29).

What is known about this topic?

- Phosphodiesterase (PDE)3 inhibitor, cilostazol inhibits agonist-induced human platelet aggregation *ex vivo* but does not prolong bleeding time, and the risk of haemorrhage associated with treatment is quite low.
- Cilostazol neither increases cAMP levels of human platelets nor inhibits shear stress-induced platelet aggregation at therapeutic concentration in the absence of Gs stimulator *in vitro*.
- Cilostazol is not appropriate for *in vitro* experiments, because it is converted into several active metabolites *in vivo*.

What does this paper add?

- We investigated the anti-platelet mechanism of a more potent and selective PDE3 inhibitor, K-134, which is a cilostazol analog but not a pro-drug.
- Therapeutic concentrations of K-134 plus a low concentration of Gs stimulator synergistically increased platelet cAMP levels and strongly suppressed high shear-dependent platelet thrombus formation initiated by interactions between GPIb/V/IX and VWF but had much lower inhibitory effects under low shear than GPIIb/IIIa inhibitor or cyclooxygenase inhibitor.

Unlike tirofiban and ASA, PDE3 inhibitor does not prolong human bleeding time, even under repeated dosing, but exhibits significant inhibitory effects on agonist-induced platelet aggregation *ex vivo* (3, 4). Considering the observed high shear stress- and Gs stimulation-dependent antiplatelet effects of PDE3 inhibitor *in vitro* (► Figs. 4, 5), it may exert *in vivo* antiplatelet activity in a shear-dependent manner when concomitant stimulation of Gs-coupled receptors is induced at the site of arterial thrombosis and ischaemia. In contrast, tirofiban and ASA inhibit platelet aggregation regardless of shear and Gs stimulation, and thus may affect physiological haemostatic plug formation. To further understand the mechanism of their low risk of bleeding, we need to explore how the local concentrations of endogenous Gs stimulators are regulated at sites of vascular perturbation.

Care should be taken when the results of our *in vitro* perfusion experiments at a high shear rate of $1,500\text{ s}^{-1}$ are interpreted into the pathological conditions *in vivo*, since the regions of arterial stenosis are exposed to much higher shear rates ranging from $1,000$ up to $10,000\text{ s}^{-1}$ (11). Nonetheless, considering the rebound phenomenon of Gs-stimulator (29), PDE3 may be a better drug-target to elevate platelet cAMP levels for the treatment of PAD (2) or secondary prevention of cerebral infarction (6) that needs long-term drug administration.

Acknowledgements

We thank Dr. A. Oda at Hokkaido University for valuable discussion and critical reading. This work was supported in part by Health and Labor Sciences Research Grants (Research on Public Essential Drugs and Medical Devices, M.H.) from the Ministry of Health, Labour and Welfare, Japan.

Conflict of Interest

The study was supported in part by a research grant from Kowa Company, Ltd. (Tokyo, Japan). H.Y. was an employee of Kowa Company, Ltd., Japan.

References

- Feijge MA, Ansink K, Vanschoonbeek K, et al. Control of platelet activation by cyclic AMP turnover and cyclic nucleotide phosphodiesterase type-3. *Biochem Pharmacol* 2004; 67: 1559–1567.
- Norgren L, Hiatt WR, Dormandy JA, et al.; TASC II Working Group. Inter-Society consensus for the management of peripheral arterial disease (TASC II). *J Vasc Surg* 2007; 45 (Suppl S): S5–67.
- Kim JS, Lee KS, Kim YI, et al. A randomized crossover comparative study of aspirin, cilostazol and clopidogrel in normal controls: analysis with quantitative bleeding time and platelet aggregation test. *J Clin Neurosci* 2004; 11: 600–602.
- Wilhite DB, Comerota AJ, Schmieder FA, et al. Managing PAD with multiple platelet inhibitors: the effect of combination therapy on bleeding time. *J Vasc Surg* 2003; 38: 710–713.
- Hiatt WR, Money SR, Brass EP. Long-term safety of cilostazol in patients with peripheral artery disease: the CASTLE study (Cilostazol: A Study in Long-term Effects). *J Vasc Surg* 2008; 47: 330–336.
- Gotoh F, Tohgi H, Hirai S, et al. Cilostazol stroke prevention study: a placebo-controlled double-blind trial for secondary prevention of cerebral infarction. *J Stroke Cerebrovasc Dis* 2000; 9: 147–157.
- Savage B, Saldívar E, Ruggeri ZM. Initiation of platelet adhesion by arrest onto fibrinogen or translocation on von Willebrand factor. *Cell* 1996; 84: 289–297.
- Savage B, Almous-Jacobs F, Ruggeri ZM. Specific synergy of multiple substrate-receptor interactions in platelet thrombus formation under flow. *Cell* 1998; 94: 657–666.
- Kasirer-Friede A, Cozzi MR, Mazzucato M, et al. Signaling through GPIb/IX/V activates alpha IIb beta 3 independently of other receptors. *Blood* 2004; 103: 3403–3411.
- Nieswandt B, Brakebusch C, Bergmeier W, et al. Glycoprotein VI but not alpha2beta1 integrin is essential for platelet interaction with collagen. *EMBO J* 2001; 20: 2120–2130.
- Jackson SP, Nesbitt WS, Westein E. Dynamics of platelet thrombus formation. *J Thromb Haemost* 2009; 7 (Suppl 1):17–20.
- Akiyama H, Kudo S, Shimizu T. The metabolism of a new antithrombotic and vasodilating agent, cilostazol, in rat, dog and man. *Arzneimittelforschung* 1985; 35: 1133–1140.
- Minami N, Suzuki Y, Yamamoto M, et al. Inhibition of shear stress-induced platelet aggregation by cilostazol, a specific inhibitor of cGMP-inhibited phosphodiesterase, *in vitro* and *ex vivo*. *Life Sci* 1997; 61: PL 383–389.
- Sudo T, Tachibana K, Toga K, et al. Potent effects of novel antiplatelet aggregatory cilostamide analogues on recombinant cyclic nucleotide phosphodiesterase isozyme activity. *Biochem Pharmacol* 2000; 59: 347–356.
- Koga Y, Kihara Y, Okada M, et al. 2(1H)-quinolinone derivatives as novel anti-arteriosclerotic agents showing anti-thrombotic and anti-hyperplastic activities. *Bioorg Med Chem Lett*. 1998; 8: 1471–1476.
- Nishiya T, Kainoh M, Murata M, et al. Reconstitution of adhesive properties of human platelets in liposomes carrying both recombinant glycoproteins Ia/IIa and Ib α under flow conditions: specific synergy of receptor-ligand interactions. *Blood* 2002; 100: 136–142.
- Shenkman B, Savion N, Dardik R, et al. Testing of platelet deposition on polystyrene surface under flow conditions by the cone and plate(let) analyzer: role of platelet activation, fibrinogen and von Willebrand factor. *Thromb Res* 2000; 99: 353–361.
- Mazzucato M, Cozzi MR, Pradella P, et al. Distinct roles of ADP receptors in von Willebrand factor-mediated platelet signaling and activation under high flow. *Blood* 2004; 104: 3221–3227.
- Tschopp TB, Baumgartner HR. Platelet adhesion and mural platelet thrombus formation on aortic subendothelium of rats, rabbits, and guinea pigs correlate negatively with the vascular PGI₂ production. *J Lab Clin Med* 1981; 98: 402–411.
- Sun B, Le SN, Lin S, et al. New mechanism of action for cilostazol: interplay between adenosine and cilostazol in inhibiting platelet activation. *J Cardiovasc Pharmacol* 2002; 40: 577–585.
- Bodnar RJ, Xi X, Li Z, et al. Regulation of glycoprotein Ib-IX-von Willebrand factor interaction by cAMP-dependent protein kinase-mediated phosphorylation at Ser 166 of glycoprotein Ib(beta). *J Biol Chem* 2002; 277: 47080–47087.
- Mazzucato M, Pradella P, Cozzi MR, et al. Sequential cytoplasmic calcium signals in a 2-stage platelet activation process induced by the glycoprotein Ibalph α mechanoreceptor. *Blood* 2002; 100: 2793–2800.
- Yap CL, Hughan SC, Cranmer SL, et al. Synergistic adhesive interactions and signaling mechanisms operating between platelet glycoprotein Ib/IX and integrin alpha IIb beta 3. *J Biol Chem* 2000; 275: 41377–41388.
- Ichinohe T, Takayama H, Ezumi Y, et al. Cyclic AMP-insensitive activation of c-Src and Syk protein-tyrosine kinases through platelet membrane glycoprotein VI. *J Biol Chem* 1995; 270: 28029–28036.
- Rynningen A, Jensen BO, Holmsen H. Role of autocrine stimulation on the effects of cyclic AMP on protein and lipid phosphorylation in collagen-activated and thrombin-activated platelets. *Eur J Biochem* 1999; 260: 87–96.
- Liu J, Pestina TI, Berndt MC, et al. The roles of ADP and TXA₂ in botrocetin/VWF-induced aggregation of washed platelets. *J Thromb Haemost* 2004; 2: 2213–2222.
- Pasini FL, Capocchi PL, Perri TD. Adenosine and chronic ischemia of the lower limbs. *Vasc Med* 2000; 5: 243–250.
- Mubagwa K, Flameng W. Adenosine, adenosine receptors and myocardial protection: an updated overview. *Cardiovasc Res* 2001; 52: 25–39.
- Sinzinger H, Silberbauer K, Horsch AK, et al. Decreased sensitivity of human platelets to PGI₂ during long-term intraarterial prostacyclin infusion in patients with peripheral vascular disease—a rebound phenomenon? *Prostaglandins* 1981; 21: 49–51.

INTRAOSSUEOUS TRANSFUSION WITH LIPOSOME-ENCAPSULATED HEMOGLOBIN IMPROVES MOUSE SURVIVAL AFTER HYPOHEMOGLOBINEMIC SHOCK WITHOUT SCAVENGING NITRIC OXIDE

Satoshi Shono,^{*†} Manabu Kinoshita,[†] Bonpei Takase,[‡] Yashiro Nogami,[§]
Shinichi Kaneda,^{||} Masayuki Ishihara,^{||} Daizoh Saitoh,^{**}
Makoto Kikuchi,^{††} and Shuhji Seki[†]

Departments of ^{*}Defense Medicine, [†]Immunology and Microbiology, [‡]Intensive Care Medicine, and [§]Surgery, National Defense Medical College, Tokorozawa; ^{||}Terumo Research Institute, Kanazawa; Divisions of ^{||}Biomedical Engineering, ^{**}Traumatology, and ^{††}Department of Medical Engineering, National Defense Medical College, Tokorozawa, Japan

Received 28 Dec 2009; first review completed 19 Jan 2010; accepted in final form 19 Apr 2010

ABSTRACT—Recently, we developed liposome-encapsulated hemoglobin (LEH), a novel cellular hemoglobin-based oxygen carrier. We hypothesized that the LEH effectively suppresses scavenging of nitrogen oxides by sequestering hemoglobin, thereby being useful for resuscitation from hemorrhagic shock, especially in prehospital settings where blood transfusion is not available. However, putting a catheter into the peripheral vessels is sometimes difficult in prehospital resuscitation, because these vessels collapse in patients with hemorrhagic shock. The intraosseous route does not collapse under such conditions. We here studied the resuscitation of severe hypohemoglobinemia following massive hemorrhage using intraosseous (intrafemur) transfusion with LEH in mice. First, we examined the effect of intravenous transfusion with LEH on the resuscitation of mice with fatal hypohemoglobinemia that was made with progressive hemodilution by blood exchanges. Despite a success in initial resuscitation without scavenging of NO_2^- or NO_3^- , LEH transfusion did not significantly improve mouse survival 72 h later as compared with red blood cell (RBC) transfusion. In other experiments, hypohemoglobinemic mice were also made with blood withdrawal and intraosseous infusion with 5% albumin. Thereafter, the mice were rescued with intraosseous transfusion of LEH or RBCs. Unlike intravenous transfusion, intraosseous transfusion with LEH (but not such transfusion with RBCs) significantly increased mouse survival without scavenging of NO_2^- or NO_3^- , presumably because LEH vesicles were much smaller than RBCs, thereby effectively flowing into the circulation from the femur. Thus, intraosseous transfusion with LEH may be a candidate strategy for efficient prehospital resuscitation from hemorrhagic shock.

KEYWORDS—Blood substitute, hemodilution, hemorrhage, resuscitation, NO_2^- , NO_3^- , TNF, erythropoietin

INTRODUCTION

Hemoglobin-based oxygen carriers (HBOCs) might be very useful for resuscitation of patients with fatal hypohemoglobinemic shock, especially in a prehospital setting where conventional blood transfusion is not available. Hemoglobin-based oxygen carriers have many advantages, such as long shelf life, not needing refrigeration and cross-matching, and reducing the risk of iatrogenic infection (1–3). Nevertheless, several clinical trials have reported that resuscitation from hemorrhagic shock using HBOCs does not seem to be very effective (4–7). We believe that one of the reasons for these unfavorable results is that hemoglobin (Hb) molecules of HBOCs might easily bind to NO when released into the vasculature, because the HBOCs used in the clinical trials had no lipid membrane, being termed *cell-free Hb* (8). Natanson et al. (7) have pointed out that this NO scavenging effect might result in systemic vasoconstriction, decreased blood flow, increased proinflammatory mediators and potent vasoconstrictors, and a loss of platelet inactivation,

creating conditions that may lead to vascular thrombosis of the heart or other organs. Therefore, development of a novel cellular HBOC that prevents direct contact between Hb and NO is an attractive goal that would limit the effects of NO scavenging.

Liposome-encapsulated Hb (LEH) was developed at the Terumo Research and Development Center (Terumo Co, Tokyo, Japan) (9, 10). Unlike cell-free Hb, LEH has a unique structure, with Hb encapsulated within a lipid bilayer membrane (liposome)—mimicking human red blood cells (RBCs)—and thereby suppressing direct contact between the Hb and NO (11). Although LEH has a lipid membrane similar to that of natural RBCs, the vesicle size of LEH is 220 nm in diameter, which is smaller than a natural RBC (9). Recently, we demonstrated that LEH transfusion is capable of rescuing rats from lethal progressive hemodilution by improving tissue hypoxia (12). In that study, we also demonstrated that LEH transfusion does not decrease the plasma nitrogen oxide levels in rats, suggesting that LEH does not have a potent NO scavenging effect. However, we did not examine the plasma NO_2^- or NO_3^- levels precisely.

In the case of prehospital hemorrhagic shock patients, it is in practice difficult to put a catheter into the peripheral vessels, because these vessels are collapsed from massive blood loss and centralization of circulating blood. Alternative transfusion routes that do not collapse even in hemorrhagic shock are necessary for effective and prompt resuscitation. The intraosseous

Address reprint requests to Manabu Kinoshita, MD, PhD, Department of Immunology and Microbiology, National Defense Medical College, 3-2 Namiki, Tokorozawa, 359-8513, Japan. E-mail: manabu@ndmc.ac.jp.

Supplemental digital content is available for this article. Direct URL citation appears in the printed text and is provided in the HTML and PDF versions of this article on the journal's Web site (www.shockjournal.com).

DOI: 10.1097/SHK.0b013e3181e46e93

Copyright © 2010 by the Shock Society

route may provide a useful means of rapidly establishing vascular access, because intraosseous infusion has been a rapid, reliable method of achieving vascular access under emergency condition in children (13–15). Therefore, we have developed the administration of a cellular-type HBOC, LEH, via the intraosseous route, and we here report that intraosseous infusion with the LEH can effectively rescue mice from hypohemoglobinemic shock without scavenging plasma NO_2^- or NO_3^- .

MATERIALS AND METHODS

Animal preparation

This study was conducted according to the guidelines of the Institutional Review Board for the Care of Animal Subjects at the National Defense Medical College, Japan. Male C57BL/6 mice (7 weeks old, 20–23 g; SLC Japan Inc, Hamamatsu, Japan) were studied.

Preparation of LEH, washed mouse RBCs, and 5% albumin solution

The LEH (TRM-645) was prepared at the Terumo Research and Development Center (Terumo Co, Tokyo, Japan). Briefly, purified human Hb solution was prepared from outdated human RBCs provided by the Japanese Red Cross, with inositol hexaphosphate as an allosteric effector, nicotinamide adenine dinucleotide as a coenzyme, and glucose, adenine, and inosine as substrates. After washing, human RBCs were hemolyzed with simultaneous virus inactivation. Subsequently, Hb was concentrated using a reverse osmosis membrane and sterilized. Thereafter, the purified Hb was adjusted to 40 to 50 mmHg of P_{50} (the oxygen partial pressure at which Hb is half saturated with oxygen) by adding inositol hexaphosphate. After adjusting the P_{50} , purified Hb was encapsulated with lipid ingredients through the use of high-speed emulsification. The surface of the encapsulating lipid membrane was then modified with 5-kd polyethylene glycol. The LEH was diluted with saline to achieve a final Hb concentration of 6 g/dL and then deoxygenated with N_2 bubbling for storage. The diameter of the LEH was approximately 220 nm. The total lipid concentration of the LEH solution was 3.9 g/dL, with the methemoglobin proportion at 6.3%. The content of lipopolysaccharide was less than 0.1 EU/mL (9, 10).

To prepare washed mouse RBCs, blood was taken from nontreated mice under ether anesthesia and added to citrate phosphate dextrose solution, which contained 2.63 g sodium citrate, 2.32 g glucose, 327 mg citric acid, and 251 mg sodium biphosphate per 100 mL.

The preservation time was less than 3 days. Before use, the preserved blood was centrifuged at 3,000g for 10 min at 4°C, washed three times with 0.9% saline, and diluted with saline to achieve a final concentration of 6 g/dL because RBC concentration has been determined to set equal oxygen transporting efficiencies for LEH and mouse RBCs (12).

Before use, human serum albumin (HSA; Kaketsuken, Kumamoto, Japan) was added to both the LEH and mouse RBC suspensions to achieve a final albumin concentration of 5 g/dL (colloid osmotic pressures, 20 mmHg) (16). Addition of HSA allows us to exclude osmotic effects during correction of hypovolemia, because precise evaluation is needed of the effects of the reagents on hypohemoglobinemic shock. The colloid infusions are usually more effective than crystalloids in restoring myocardial blood flow and oxygen transport after acute hemorrhage (17). A 5% HSA solution (5 g/dL) was also prepared.

Hypohemoglobinemic shock by blood exchange and intravenous fluid resuscitation

Under ether anesthesia, a plastic catheter was put into the mouse superior vena cava. Thereafter, 0.2 mL of blood was withdrawn, and immediately, isovolumetric 5% albumin was administered via catheter. This blood exchange was repeated until the mice died to establish a lethal hypohemoglobinemic shock model. No mice could survive beyond 8 such blood exchanges. Therefore, after 7 exchanges of blood, the mice received intravenous administration with 0.5 mL of LEH, 5% albumin solution, or washed RBCs.

The effect of additional intravenous LEH or RBC transfusion after first intravenous transfusion

The mice received intravenous administration with 0.5 mL of LEH ($n = 20$) or washed RBCs ($n = 10$) 6 h after blood exchange and the first intravenous transfusion.

Intraosseous or intravenous fluid resuscitation following massive hemorrhage

To establish an intraosseous infusion route in mice, the femur was punctured with a 25-gauge needle followed by laparotomy under deep ether anesthesia. Immediately after infusion with indocyanine green (ICG; Daiichi, Tokyo, Japan) via this intraosseous route, the inferior vena cava was stained with ICG (indicated by arrow, Fig. 1), suggesting a rapid flow into the systemic circulation.

To produce hemorrhagic shock in mice, a 27-gauge needle was put into the femoral vein, and 0.8 mL of blood was withdrawn. The mean arterial pressure (MAP) showed approximately 40 mmHg. Subsequently, the femur (opposite side) was punctured with a 25-gauge needle, and then, 1 mL of 5% albumin was administered intraosseously. This intraosseous administration with albumin effectively rescued the subject mice. Five minutes after initial resuscitation, 0.3 mL of blood was additionally withdrawn, and subsequently, 1 mL of LEH, 5% albumin, or washed RBCs was also administered via the intraosseous route or the intravenous route (femoral vein).

Measurement of Hb in mouse blood samples containing LEH and RBC

Hemoglobin concentration in LEH could not be accurately determined, because the liposome capsules interfered with the spectrophotometric measurement

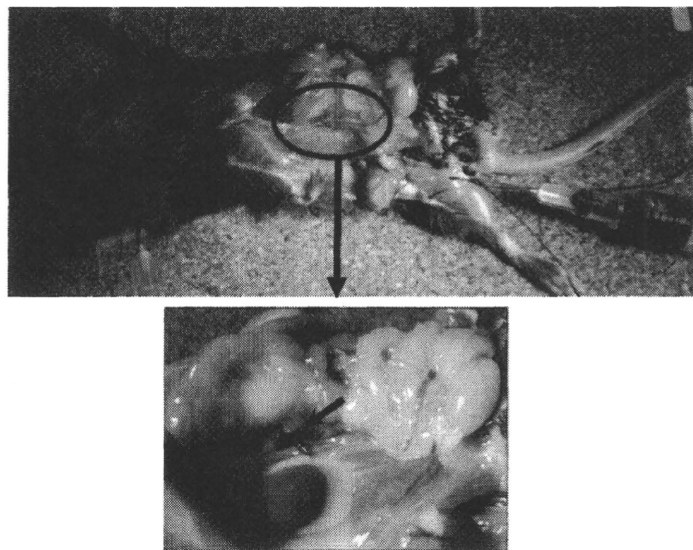


Fig. 1. Indocyanine green was administered by intraosseous infusion via the right femur. The circle shows the abdominal inferior vena cava, which was stained with ICG (arrow).

of Hb absorbance. However, the measured Hb concentration in the LEH solution, as determined by the Erma PCE 170 hematology analyzer, was 5-fold higher than the actual concentration that was determined when using a specific enzyme-linked immunosorbent assay for human Hb during the production of LEH (see Figure, Supplemental Digital Content 1, <http://links.lww.com/SHK/A51>). We then estimated the actual Hb concentration in the LEH-transfused mouse samples based on the measured Hb concentration of each sample. First, the mouse RBC-derived Hb concentration in an LEH-mixed blood sample was estimated by reproducing an RBC suspension that had the same hematocrit as the sample. We then measured its Hb concentration, because the hematocrit in the LEH-mixed blood sample reflected the concentration of the mouse RBCs, given that the mean corpuscular volume essentially remained unchanged in all of the mice during the experiment. The LEH-derived Hb concentration was then obtained by subtracting the mouse RBC-derived Hb concentration from the measured Hb concentration, with the determination of the actual LEH-derived Hb concentration calculated by dividing the obtained LEH-derived Hb concentration by 5. The total concentration of Hb in the samples containing a mixture of RBCs and LEH was determined by adding the estimated LEH-derived Hb concentration and the mouse RBC-derived Hb concentration (12).

Measurements of plasma NO_2^- , NO_3^- , TNF, and erythropoietin levels

Collected blood samples were immediately heparinized and then centrifuged at 50,000g at 4°C for 20 min to remove the LEH particles. The plasma supernatant was stored at -80°C until assay. For NO determination, the plasma was mixed with methanol (1:1) followed by centrifugation at 10,000g at 4°C for 10 min to remove proteins, and the supernatant was used for measurement of plasma NO_2^- and NO_3^- levels. Determinations of plasma NO levels were performed on a high-performance liquid chromatography-Griess system (ENO-20; Eicom, Kyoto, Japan). This instrument applied a post-column derivatization method with Griess reagent for nitrite and nitrate detection. At first, nitrite and nitrate are separated from the other substances on a separation column. Thereafter, nitrite reacts with the Griess reagent and generates diazo compounds. The separated nitrate is reduced by a cadmium-copper column to react with the Griess reagent. The level of diazo compounds is then measured by a visible detector installed in a column oven at high stability and sensitivity. The detection limits and sensitivities were 0.01 μM for both NO_2^- and NO_3^- . The loading volume of plasma was 10 μL . The area under the curve of each chromatogram was calculated for quantitative analysis of NO_2^- and NO_3^- , using the analyzing software PowerChrom (AD Instrument Co, Ltd, Tokyo, Japan). Plasma samples were also tested with enzyme-linked immunosorbent assay kits for TNF (BD Pharmingen) and mouse Epo immunoassay (R&D Systems).

Operation procedure and samples analysis

All operations are performed with a microscope (SZ6045; Olympus Optical, Tokyo, Japan) and microsurgical technique. If the failure of the first fluid resuscitation or technical problems were found, the samples were removed from the data. The reason of failure was mainly unexpected bleeding or extravasation such as intramuscular infusion or subcutaneous infusion.

Statistical analysis

Statistical analyses were performed using the Stat View 4.02J software package (Abacus Concepts, Berkeley, Calif). Survival rates were compared by the Wilcoxon signed rank test. Statistical evaluations between two groups were compared using the Student *t* test, and any other statistical evaluations were compared using one-way ANOVA, followed by the Bonferroni post hoc test. Data are presented as the mean \pm SE. *P* < 0.05 was considered to be statistically significant.

RESULTS

Fatal hypohemoglobinemia induced by blood exchange

Blood exchange was performed on mice (*n* = 15) by a 0.2-mL blood withdrawal and an isovolumetric intravenous injection of 5% albumin. The mice repeatedly received this blood exchange until they died. No mice survived beyond eight iterations of this blood exchange (Fig. 2A). Mean arterial pressure was decreased to 40 mmHg in the mice after seven exchanges of blood (Fig. 2B), and Hb concentration was decreased to approximately 5 g/dL because of progressive hemodilution, suggesting a fatal hypohemoglobinemia (Fig. 2C). Hematocrit, RBC count, platelet, and WBC counts were also decreased with hemodilution (Fig. 2, D-G).

Resuscitation of fatal hypohemoglobinemia by intravenous transfusion with LEH or RBCs

After seven exchanges of blood, the mice were intravenously transfused with 0.5 mL LEH (*n* = 20), 5% albumin (*n* = 20), or washed RBCs (*n* = 20). Although no mice were rescued by albumin transfusion, all of the LEH- and RBC-transfused mice recovered from hypohemoglobinemia within 6 h (normally fatal), suggesting a success in initial resuscitation (Fig. 3A). Both transfusions with LEH and RBCs promptly restored MAP to 70 mmHg from 30 mmHg. Nevertheless, the survival rate of LEH-transfused mice gradually decreased to 25% at 36 h, whereas RBC-transfused mice sustained a higher survival rate (Fig. 3A). Both LEH-transfused and RBC-transfused mice showed an increase in Hb concentration immediately after transfusion (at 5 min) (Fig. 3B). However, LEH-transfused mice did not show an increase in hematocrit or

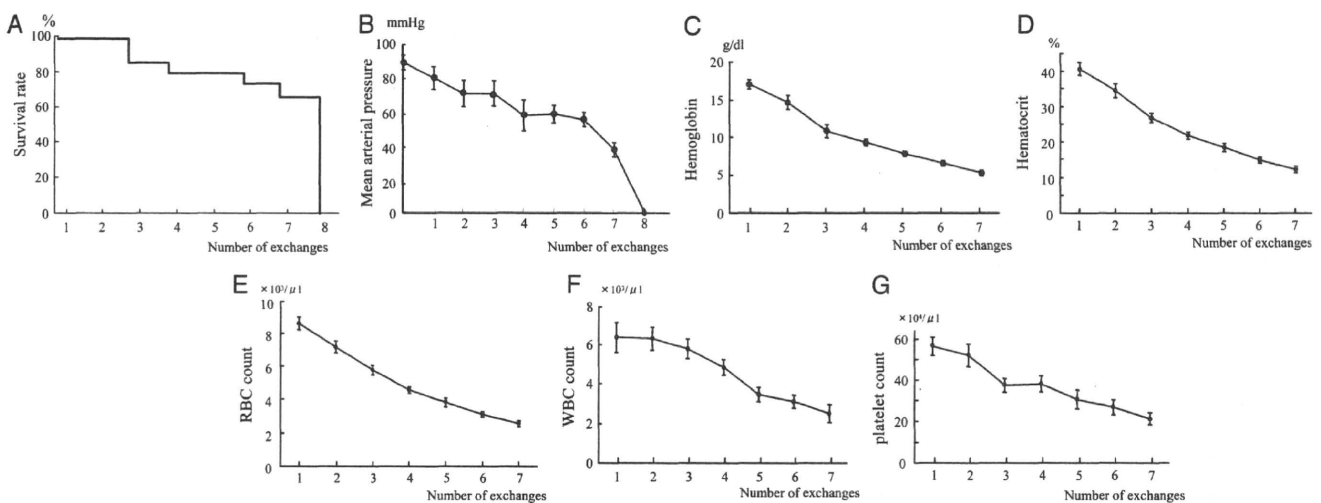


Fig. 2. Data on the survival (A), mean arterial pressure (B), Hb level (C), hematocrit (D), RBC count (E), WBC count (F), and platelet count (G) of mice undergoing progressive hemodilution. The mice repeatedly had 0.2 mL of blood withdrawn followed by isovolumetric intravenous injection with 5% albumin. Data are mean \pm SE from 15 mice.

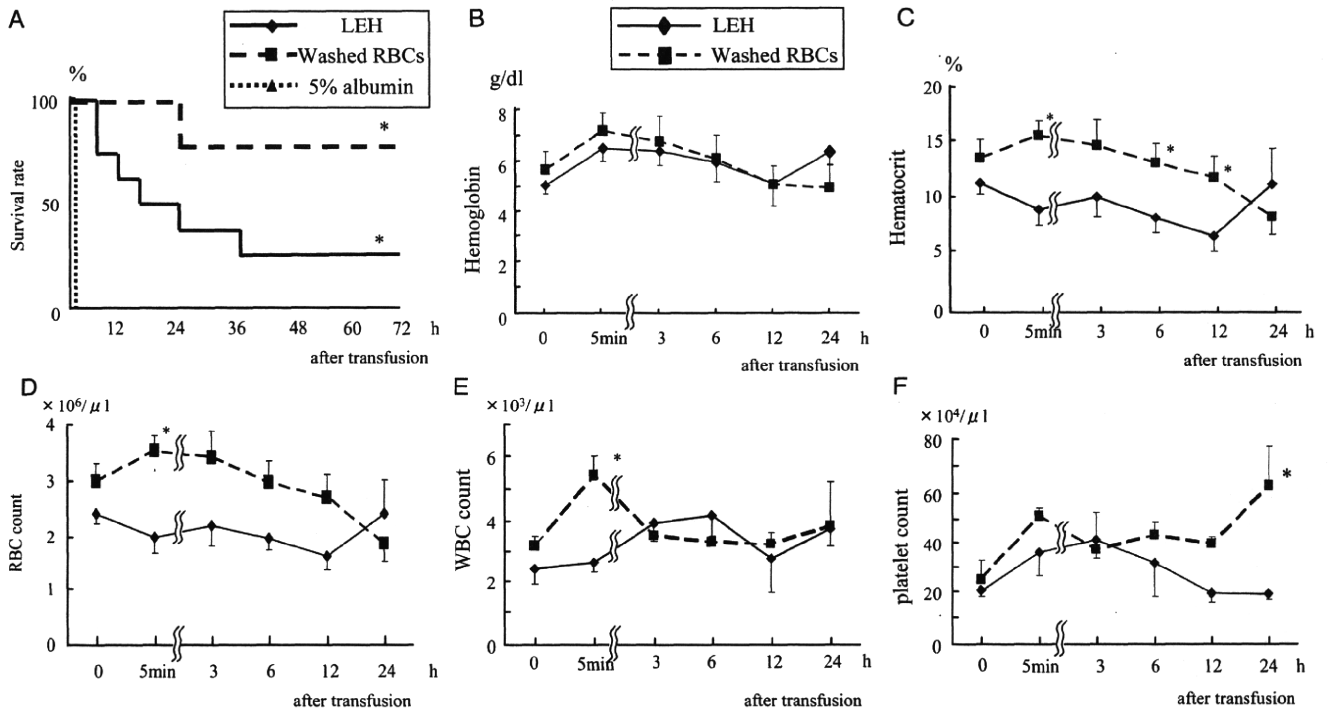


Fig. 3. The effect of resuscitation fluid on the survival (A), Hb level (B), hematocrit (C), RBC count (D), WBC count (E), and platelet count (F) in mice with fatal hypohemoglobinemia. Fatal hypohemoglobinemia was induced in the mice by seven 0.2-mL exchanges of blood. Thereafter, the mice were treated by intravenous transfusion with 0.5 mL LEH, 5% albumin, or washed RBCs. Data are mean \pm SE from 20 mice in each group. * $P < 0.05$ vs. the other groups.

RBC count after transfusion (although RBC-transfused mice did), because the present hematology analyzer cannot detect a vesicle the size of LEH (200 nm) (Fig. 3, C and D). White blood cell count was transiently increased in the mice immediately after RBC transfusion but not after LEH transfusion (Fig. 3E). The platelet count was also increased 24 h after RBC transfusion but not after LEH transfusion (Fig. 3F). These findings suggest the possibility that hematologic alterations induced by massive blood transfusion do not occur after massive LEH transfusion.

Serum TNF and plasma NO levels after resuscitation by intravenous transfusion with LEH or RBCs

Serum TNF levels were increased in the mice with repeated blood exchanges, whereas those levels decreased after transfusion with either RBCs or LEH (Fig. 4A); no statistical difference in the change in TNF levels was observed between the

two groups. Although plasma NO_2^- levels were not increased in the mice during the blood exchanges, they were promptly increased after RBC transfusion. Plasma NO_2^- levels also gradually increased in the mice after LEH transfusion, but the increase was quite different from that after RBC transfusion (Fig. 4B). However, no obvious decrease in the plasma NO_2^- levels was observed after LEH transfusion. Plasma NO_3^- levels were slightly decreased in both groups not only during the blood exchanges but also after RBC transfusion (Fig. 4C). These findings suggest that LEH transfusion does not induce a potent NO scavenging effect in the subject mice.

The effect of additional intravenous LEH or washed RBC transfusion after first intravenous transfusion

We examined the effect of additional intravenous LEH transfusions (n = 20) or washed RBC transfusions (n = 10) 6 h after first transfusion. Twenty percent of the mice died within

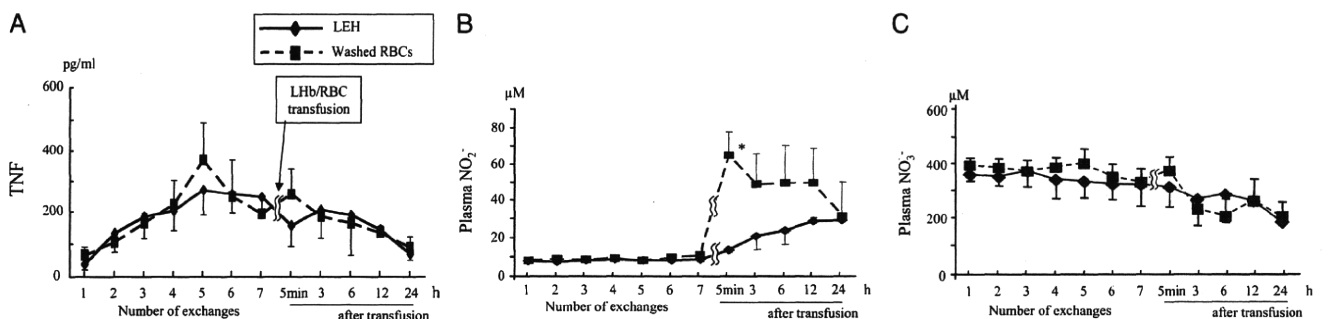


Fig. 4. The change in serum TNF (A), plasma NO_2^- (B), and NO_3^- (C) levels in the mice during the blood exchanges and after resuscitation by LEH or washed RBC transfusions, as described in Figure 2. Data are mean \pm SE from 10 mice in each group. * $P < 0.05$ vs. the other group.

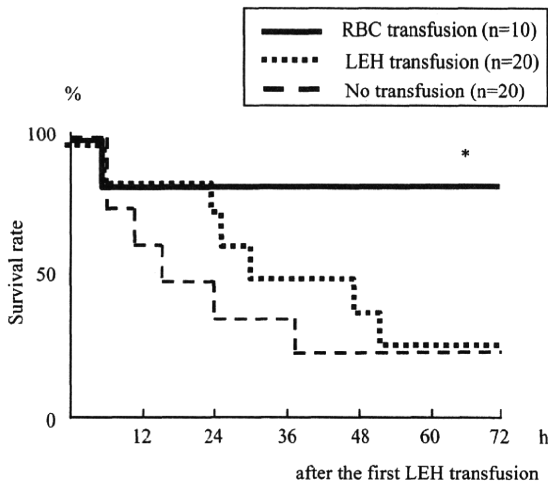


Fig. 5. Survival of repeated LEH transfusion and RBC transfusion after LEH transfusion in mice with fatal hypohemoglobinemia. Fatal hypohemoglobinemia was induced in the mice by seven 0.2-mL exchanges of blood. Thereafter, the mice were treated by intravenous transfusion with 0.5 mL LEH or washed RBCs 6 h after intravenous transfusion with 0.5 mL LEH. Data are mean \pm SE in each group. * $P < 0.05$ vs. the other groups.

6 h and did not receive LEH or washed RBC transfusion. The remained mice all survived after an additional washed RBC administration. The survival of mice receiving an additional LEH transfusion extended to 24 h, but the survival rate had decreased to same level as a single LEH administration at 48 h (Fig. 5).

Resuscitation of massive hemorrhage model by intrasosseous transfusion with LEH or RBCs

Mice had 0.8 mL of blood withdrawn and subsequently were intrasosseously infused with 1 mL of 5% albumin. All subjected mice survived the first hemorrhage with this treatment, although no mice survived without any fluid resuscitation. Next, those mice had 0.3 mL of additional blood withdrawn and then were intrasosseously transfused with 1 mL of either LEH ($n = 10$), 5% albumin ($n = 10$), or RBCs ($n = 10$). Immediately after the second withdrawal, Hb concentration was decreased to approximately 6 g/dL in the subject mice, suggesting a severe hypohemoglobinemia. Intrasosseous infusion with 5% albumin rescued approximately 30% of the subjected mice after the second withdrawal; however, intrasosseous transfusion with LEH significantly increased mouse survival (Fig. 6A). Unexpectedly, intrasosseous transfusion

with RBCs did not effectively increase mouse survival (Fig. 6A). These results suggest the following two important findings. First, intrasosseous transfusion with RBCs may not be effective for serious massive hemorrhage in mice. Second, intrasosseous transfusion with LEH might be very effective for even such a serious hemorrhage.

Consistent with survival rates, intrasosseous transfusion with LEH significantly increased Hb concentration in the mice compared with either 5% albumin or RBCs (Fig. 6B), suggesting that LEH can effectively flow into the systemic circulation from the femur, unlike RBCs. Intrasosseous transfusion with either LEH or 5% albumin increased neither RBC count nor hematocrit in the mice 1 h after transfusion, although intrasosseous transfusion with RBCs gave such an increase (but slight) (Fig. 6, C and D), because the hematology analyzer cannot detect the LEH vesicles.

Serum TNF, erythropoietin, and plasma NO levels after intrasosseous transfusion

Intrasosseous transfusion with RBCs increased serum TNF levels in mice immediately after the transfusion (at 5 min) and kept them higher levels, in contrast to intrasosseous transfusion with LEH or 5% albumin (Fig. 7A). Because intrasosseous transfusion with LEH tended to increase hematocrit and RBC count beyond 48 h after the transfusion (Fig. 6, C and D), we examined the effect of LEH on the induction of erythropoietin, which stimulates RBC production in the bone marrow. Erythropoietin levels were increased after intrasosseous transfusion and peaked at 12 h in all three groups. However, there was no significant difference in the erythropoietin levels among the three groups (Fig. 7B), suggesting that LEH does not affect erythropoietin-stimulated RBC production in the bone marrow. No significant decreases in the plasma NO_2^- or NO_3^- levels were observed in the mice after intrasosseous transfusion with LEH relative to levels with 5% albumin or RBCs (Fig. 7C and D), suggesting that LEH does not have a potent NO scavenging effect, similar to our results for intravenous transfusion.

Resuscitation of massive hemorrhage model by intravenous transfusion with LEH or RBCs

Finally, we examined the effect of intravenous transfusion with LEH or RBCs on the mouse survival in this hemorrhage model. After the second blood withdrawal, the mice were intravenously transfused with LEH ($n = 10$), 5% albumin ($n = 10$),

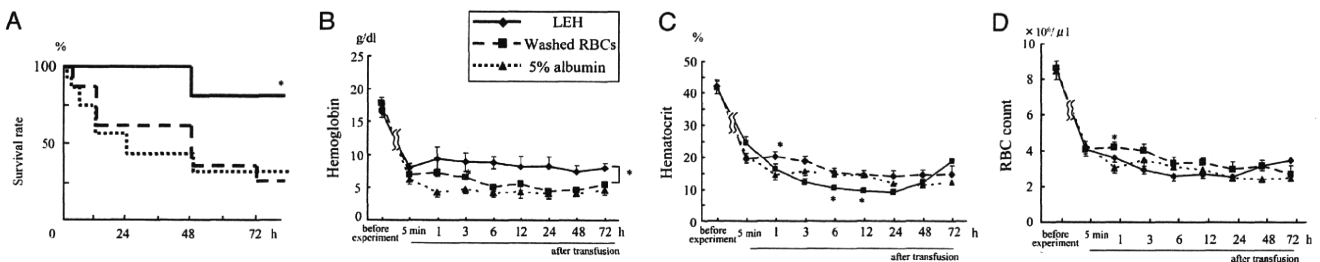


Fig. 6. The effect of intrasosseous transfusion on the survival (A), Hb level (B), hematocrit (C), and RBC count (D) in mice. The mice had 0.8 mL of blood withdrawn followed by intrasosseous infusion with 1 mL of 5% albumin. Subsequently, they had 0.3 mL of additional blood withdrawn. Thereafter, the mice were treated by intrasosseous transfusion with 1 mL of either LEH, 5% albumin, or washed RBCs. Data are mean \pm SE from 10 mice in each group. * $P < 0.05$ vs. the other groups.

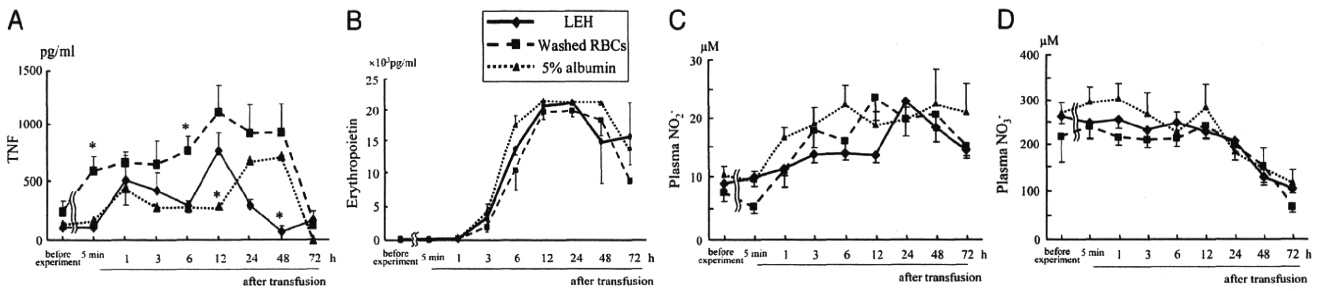


FIG. 7. The change in serum TNF (A), erythropoietin (B), plasma NO_2^- (C), and NO_3^- (D) levels in mice after intrasosseous transfusion. The mice had blood withdrawn and intrasosseous infusion as described in Figure 5. The changes in serum/plasma mediators after intrasosseous transfusion with LEH, 5% albumin, or washed RBCs are shown. Data are mean \pm SE from 10 mice in each group. * $P < 0.05$ vs. the other groups.

or RBCs (n = 10). As expected, intravenous transfusion with RBCs effectively increased mouse survival as well as that with LEH (Fig. 8A). Consistently, intravenous transfusion with RBCs significantly increased Hb concentration, hematocrit, and RBC count in the mice after transfusion (Fig. 8, B–D), suggesting an effective and rapid replenishment of RBC in the systemic circulation.

DISCUSSION

Intrasosseous transfusion with LEH more effectively rescued mice from fatal hemorrhage without scavenging NO than did intrasosseous transfusion with RBCs. The present study clearly demonstrates the advantage of LEH, relative to conventional blood transfusion, as a blood substitute in resuscitation from massive hemorrhage in prehospital environment.

Despite many physiological modifications of Hb (2), cell-free Hbs reportedly increased the risk of myocardial infarction and death in a meta-analysis of the data from the clinical trials (7). These disadvantages of cell-free Hbs are thought to derive from their vasopressor effect, resulting from NO scavenging (2, 9, 10). Thus, NO scavenging induced by cell-free Hbs must be one of the most serious and fundamental adverse effects of the resuscitation of patients with hemorrhagic shock. Cross-linkage and/or polymerization of cell-free Hbs seem to be insufficient to prevent NO scavenging, because basically they do not have a structure like a cellular membrane, which may be indispensable in preventing direct contact between Hb and NO.

It is noteworthy that the current encapsulated Hb induced neither an NO scavenging effect nor elevation of serum TNF in mice after either intravenous or intrasosseous transfusion. Mice receiving intravenous or intrasosseous transfusion with LEH

showed no marked decrease in the plasma NO_2^- or NO_3^- levels. Although the mice transfused with RBCs also showed no decrease in NO_3^- levels, NO_2^- levels were promptly increased after intravenous RBC transfusion. Regarding this, it has been reported that blood pressure decreased after iso-volemic exchange transfusion with RBCs, in which increased blood viscosity induced shear stress-mediated production of NO in endothelial cells, leading to vasodilatation and hypotension (18–20). We speculate that a similar mechanism may explain the increased NO production in the first RBC infusion model. This is a first report measuring the plasma NO_2^- and NO_3^- levels after HBOC transfusion and, more importantly, showing a significant protection from both NO_2^- and NO_3^- scavenging effects induced by HBOC. Our novel HBOC, namely LEH, might have a potential for rescuing hemorrhagic shock patients without NO scavenging.

The intrasosseous infusion route is reported to be a viable means of blood transfusion in a nonhemorrhagic swine model (21). Crystalloid infusion via the intrasosseous route with a fixed (not rapid) rate was as effective as peripheral and central intravenous accesses for reversible hemorrhagic shock (22). However, the tortuous vascular architecture in the bone marrow might cause substantial hydraulic resistance to rapid infusion with fluid. The flow volume of intrasosseous infusion with RBCs was significantly smaller than for saline under both normal gravitational and 300-mmHg pressures (23). Thus, rapid transfusion with RBCs via the intrasosseous route may not be effective in rescuing the host from hemorrhagic shock. Therefore, crystalloid or colloid fluid infusion via intrasosseous route is usually used for hypovolemic shock. However, asanguineous fluid cannot rescue the patients from fatal severe

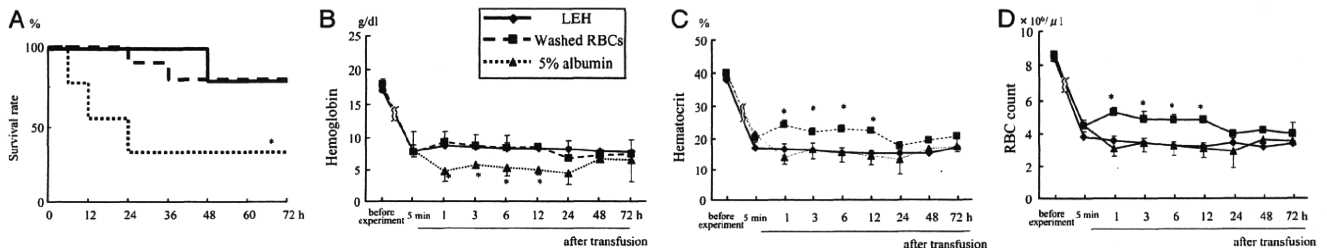


FIG. 8. The effect of intravenous transfusion on the survival (A), Hb level (B), hematocrit (C), and RBC count (D) in mice. The mice had 0.8 mL of blood withdrawn from the femoral vein and intrasosseous infusion with 1 mL of 5% albumin. Subsequently, they had 0.3 mL of additional blood withdrawn. Thereafter, the mice were treated by intravenous transfusion with 1 mL of either LEH, 5% albumin, or washed RBCs. Data are mean \pm SE from 10 mice in each group. * $P < 0.05$ vs. the other groups.

anemia resulting from massive Hb loss and tissue hypoxia (12), and administration of an oxygen carrier including LEH or RBCs is preferable for resuscitation in that situation.

Thus, we tried to establish the simple model with intraosseous infusion after blood exchange. However, this model did not succeed because approximately 90% of the animals were dropped because of anesthetic problems, unexpected cardiac arrest, or bleeding when attempting the intraosseous route. The second model tried to reproduce resuscitation in a clinical situation when another hemorrhage occurs after adequate asanguineous infusion for an initial hemorrhage. Whereas approximately 32% of the original Hb remained after blood exchange and transfusion in the first dilution model, 40% of original Hb remained in the second model, which may explain the fact that the mouse survival after intraosseous albumin infusion was better than intravenous albumin transfusion.

Intraosseous transfusion with LEH significantly increased the survival of and the Hb levels in mice above those seen with RBCs. Because the size of the LEH vesicle is about 220 nm, which is 1/30 to 1/40 the size of a natural mouse RBC, the influx of LEH from the femur to the systemic circulation might be better than RBC influx, thereby improving mouse survival. Furthermore, the biconcave shape, size, and deformability of natural RBCs might be appropriate for passing quickly through capillaries, but perhaps not through the tortuous vascular architecture in the bone marrow. The round shape, smaller size, and elastic hardness of LEH vesicles may be more suitable for the intraosseous route. Extravasation of infusions and compartment syndrome occasionally occur in intraosseous infusion and may be associated with major morbidity. When we intraosseously transfused RBC into the mice at high pressure, extravasation of RBCs was sometimes observed around the inserting site by pressure infusion. Extravasation occurred more frequently after RBC transfusion than after LEH transfusion. Interestingly, TNF levels after intraosseous RBC transfusion were higher than those after LEH or 5% albumin treatment. Because washed RBCs cannot pass through the tortuous vascular architecture in the bone marrow smoothly, activated bone marrow macrophages may phagocytose trapped RBCs and produce TNF.

As expected, intravenous transfusion with RBCs effectively rescued the mice from fatal hypohemoglobinemia, whereas intravenous transfusion with LEH eventually could not rescue more than half of the mice (although it could rescue most of them within several hours). Some investigators have pointed out similar problems, in that the effective period of cell-free Hb is not very long (24). A clinical report on a bovine-derived Hb solution (HBOC-201; Hemopure, OPK Biotech, Cambridge, Mass) in South Africa has demonstrated that some patients presented severe anemia again 24 to 36 h after the initial administration to relieve life-threatening symptoms of anemia (24). Although mice intravenously transfused with LEH showed a change in Hb levels similar to that of mice transfused with RBCs, their survival rates were quite different. Liposome-encapsulated hemoglobin may lose its function as an oxygen carrier soon after transfusion. The functional half-life of LEH has been reported as approximately 6 h in mice (25). Although the present LEH has a long circulation time

achieved by modification of the liposomal surface with hydrophilic polymer, it was reported that the functional half-life (the period to a reduction by half of actual oxygen transport efficiency) seems to be shorter than natural Hb half-life because of methemoglobin generation (10, 25, 26). Methemoglobin formation might be one of the reasons why the LEH-transfused mice showed lower survival rates than did RBC-transfused mice despite similar Hb levels. However, transfusion with LEH saved mice for 6 h, although no mice were rescued by albumin transfusion. If survival is extended beyond 6 h, the possibility of the medical team rescuing the patient increases. Red blood cell transfusion after resuscitation with LEH may improve the survival of hypohemoglobinemic shock patients. In addition, the half-life of LEH in rat and monkey was about 10 and 70 h, respectively; therefore, a longer half-life of LEH could be anticipated in humans (10).

The present study indicates a need for transfusion with an oxygen carrier after conventional fluid resuscitation in situations of uncontrolled massive hemorrhage that can lead to fatal hypohemoglobinemia. In a hospital environment, intraosseous infusion is not needed except in special situations, because the medical staff can insert a central venous catheter for transfusion. In a prehospital environment such as a battlefield or in a confined space in disaster situations, however, sometimes only the intraosseous route will be available. If LEH can be administered to patients via the intraosseous route, resuscitation using oxygen-carrying fluid can be performed under critical conditions without special training or medical expertise.

REFERENCES

- Manning JE, Katz LM, Brownstein MR, Pearce LB, Gawryl MS, Baker CC: Bovine hemoglobin-based oxygen carrier (HBOC-201) for resuscitation of uncontrolled, exsanguinating liver injury in swine. Carolina resuscitation research group. *Shock* 13:152-159, 2000.
- Squires JE: Artificial blood. *Science* 295:1002-1005, 2002.
- Johnson T, Arnaud F, Dong F, Philbin N, Rice J, Asher L, Arrisueno M, Warndorf M, Gurney J, McGwin G, et al.: Bovine polymerized hemoglobin (hemoglobin-based oxygen carrier-201) resuscitation in three swine models of hemorrhagic shock with militarily relevant delayed evacuation—effects on histopathology and organ function. *Crit Care Med* 34:1464-1474, 2006.
- Kasper SM, Walter M, Grune F, Bischoff A, Erasmi H, Buzello W: Effects of a hemoglobin-based oxygen carrier (HBOC-201) on hemodynamics and oxygen transport in patients undergoing preoperative hemodilution for elective abdominal aortic surgery. *Anesth Analg* 83:921-927, 1996.
- Schubert A, O'Hara JF Jr, Przybelski RJ, Tetzlaff JE, Marks KE, Mascha E, Novick AC: Effect of diaspirin crosslinked hemoglobin (DCLHb HemAssist) during high blood loss surgery on selected indices of organ function. *Artif Cells Blood Substit Immobil Biotechnol* 30:259-283, 2002.
- Kerner T, Ahlers O, Veit S, Riou B, Saunders M, Pison U: DCL-Hb for trauma patients with severe hemorrhagic shock: the European "on-scene" multicenter study. *Intensive Care Med* 29:378-385, 2003.
- Natanson C, Kern SJ, Lurie P, Banks SM, Wolfe SM: Cell-free hemoglobin-based blood substitutes and risk of myocardial infarction and death: a meta-analysis. *JAMA* 299:2304-2312, 2008.
- Stern S, Rice J, Philbin N, McGwin G, Arnaud F, Johnson T, Flournoy WS, Ahlers S, Pearce LB, McCarron R, et al.: Resuscitation with the hemoglobin-based oxygen carrier, HBOC-201, in a swine model of severe uncontrolled hemorrhage and traumatic brain injury. *Shock* 31:64-79, 2009.
- Ogata Y, Goto H, Kimura T, Fukui H: Development of neo red cells (NRC) with the enzymatic reduction system of methemoglobin. *Artif Cells Blood Substit Immobil Biotechnol* 25:417-427, 1997.
- Kaneda S, Ishizuka T, Goto H, Kimura T, Inaba K, Kasukawa H: Liposome-encapsulated hemoglobin, tm-645: current status of the development and important issues for clinical application. *Artif Organs* 33:146-152, 2009.
- Sakai H, Sou K, Horinouchi H, Kobayashi K, Tsuchida E: Haemoglobin-vesicles as artificial oxygen carriers: present situation and future visions. *J Intern Med* 263:4-15, 2008.